APPLICATION OF ELECTROSPRAY MASS SPECTROMETRY TOWARD SEMI-AUTOMATED KINASE INHIBITOR SCREENING

APPLICATION OF ELECTROSPRAY MASS SPECTROMETRY TOWARD SEMI-AUTOMATED KINASE INHIBITOR SCREENING

BY

IVAN PARTSERNIAK

A Thesis

Submitted to the School of Graduate Studies in Partial fulfillment

of the Requirements for the Degree

Master of Science

McMaster University

MASTER OF SCIENCE (2007)

McMaster University

(BIOCHEMISTRY)

Hamilton, Ontario, Canada

TITLE: Application of Electrospray Mass Spectrometry Toward Semi-Automated Kinase Inhibitor Screening

Author: Ivan Partserniak, B.Sc (McMaster University)

Supervisor: Dr. John D. Brennan

ABSTRACT

Multi-site phosphorylation of protein targets by specific kinases is a common event used to propagate biological messages through signal transduction pathways in the context of the cellular environment and is a vital regulatory mechanism for many metabolic processes. Recent advances in the study of the protein glycogen synthase kinase-3 (GSK-3) have shed some light on the intricate role this enzyme plays within the framework of mammalian cellular metabolism. Abnormal behaviour of GSK-3 profoundly impacts cellular function, and is implicated in Alzheimer's disease and the development of Type II Diabetes. A key issue in assaying the activity of GSK-3 is the ability to distinguish between singly and multiply phosphorylated substrates, as this enzyme has the ability to selectively phosphorylate a previously phosphorylated (primed) substrate. Given the serious nature of the disorders caused by the dysfunction of this kinase, high throughput screening of specific inhibitors from compound libraries is urgently needed. Unfortunately, many of the currently existing kinase screening technologies are geared towards monitoring single phosphorylation events and thus, are not be amenable to effective assaying of multiply phosphorylated substrates.

In this thesis, a novel, solution-based assay method based on electrospray ionization-tandem mass spectrometry (ESI-MS/MS) is developed as a platform for inhibitor screening with full consideration being given to the specific nature of GSK-3 substrates and products. The semi-automated application of this assay is possible using an in-line autosampler, and is shown to be a potentially effective means for screening primed binding site inhibitors from compound mixtures, with subsequent deconvolution performed to isolate the effective molecule. Optimization of the MS-based assay required

significant alterations in buffer conditions compared to those used in the standard GSK-3 radioassay based on γ-^{32}P ATP, owing to the inability of electrospray ionization to tolerate high buffer concentrations. Preliminary screening of mixtures was demonstrated, and expansion to screening of large compound libraries consisting of previously untested compounds and natural product extracts should be possible.

To investigate the adaptation of the GSK-3 MS/MS assay to allow mixture deconvolution, a preliminary study was performed on the utilization of sol-gel technology for entrapment of GSK-3 to develop a solid-phase affinity assay for pull-down of bioactive ligands identified in enzyme activity assays. This method requires the preservation of enzyme function within the silica matrix, which has not been previously demonstrated for GSK-3. The sol-gel entrapment of GSK-3, however, proved to be problematic. Implementation of a flow-through assay using immobilized GSK-3 was hampered by issues such as non-specific adsorption of the cationic substrate and inhibitors, owing to electrostatic interactions with the anionic silica matrix used for enzyme entrapment. Future work aimed at further developing and optimizing the sol-gel materials and processing methods are proposed.

ACKNOWLEDGEMENTS

I acknowledge my supervisor, Prof. John D. Brennan for all the inspiring guidance and support during the last two years. Dr. Fred Capretta, Dr. Geoff Werstuck, Dr. Travis Besanger and Dr. Richard Hodgson are greatly appreciated for their helpful assistance and suggestions for my research projects.

Moreover, I would like to extend my gratitude to all the members in the Brennan group for their friendly and interesting discussions with me over the last two years. I would also like to thank Dr. Brennan for his valuable time to go through this thesis and provide advice for revision.

TABLE OF CONTENTS

LIST OF TABLES AND FIGURES

Figure 1.3. Medically relevant drug development for GSK-3β disorders must be selective in deactivating only the priming phosphorylation site - the binding site of glycogen synthase. Inhibition of the active site is undesirable, as it can deregulate cellular processes (Figure originally published in Cohen, P. and Frame, S., 2001, *Nat. Rev. Mol. Cell Biol.*[4]).

Figure 1.4. Sol-gel based method for inhibitor screening using IMER/MS technology. All mobile phases and samples contain an identical concentration of substrate, while inhibitors are 1) introduced by pump B, either through loading directly into reservoir of pump B (top) or 2) through an autosampler loop (bottom). The sol-gel column immobilizes the enzyme, allowing for interaction with multiple inhibitors. The effect of the inhibitors on substrate/product signal is monitored via ESI-MS. The first method is designed for quantitative analysis of identified inhibitors, while the second method is utilized for automated screening of multi-compound mixtures (Figure originally published in Hodgson, R.J. *et al.*, 2005, *Anal. Chem.*[36]).

Figure 2.1. The effect of Mg^{2+} ions on GSM Q1 signal. 62.5 μM GSM in 6 mM NH_4OAc with 0, 0.8, 1.6, 4 and 8 mM MgOAc were infused into the ESI-MS at 5 μL/min via the syringe pump. GSM signal to noise ratio (top); S/N normalized to 0 mM MgOAc control (bottom).

Figure 2.2. ^{32}P ATP radio assay of GSK-3β activity in solution as a function of Mg^{2+} and buffer concentrations. 0 – 2.5 mM MgOAc concentration assay (in 2 mM MOPS) (top) and 1 – 21 mM NH_4OAc concentration assay (with 0.8 mM MgOAc) (bottom).

Figure 2.3. Time based ^{32}P ATP GSK-3β activity assay with 6 mM NH_4OAc/0.8 mM MgOAc, pH 7.4 and 52.5 nM GSK-3β as positive control (red) and assay with 6 mM

NH_4OAc/0.8 mM MgOAc, pH 7.4 and no enzyme as negative control (blue).

Figure 2.4. GSM Q1 (top) and MS2 (bottom) signal analysis (P = Parent/D = Daughter ion). 62.5 μM GSM in 6 mM NH_4OAc/0.8 mM MgOAc, pH 7.4 infused at 5 μL/min via the syringe pump.

Figure 2.5. GSM & pGSM Q1 signal analysis as a function of GSK-3β concentration. Reaction enzyme concentration: 0 nM GSK-3β (top), 52.5 nM GSK-3β (middle) and 525 nM GSK-3β (bottom). 62.5 μM GSM, 125 μM ATP and 6 mM NH_4OAc/0.8 mM MgOAc, pH 7.4 buffer were used. All reactions were infused directly at 5 μL/min via the syringe pump.

Figure 2.6. pGSM Q1 (top) and MS2 (bottom) signal analysis (P = Parent ion, D = Daughter ion). A quenched reaction solution initially containing 62.5 μM GSM, 125 μM ATP and 52.5 nM GSK-3β in 6 mM NH_4OAc/0.8 mM MgOAc, pH 7.4 was infused at 5 μL/min via the syringe pump.

Figure 2.7. GSK-3β solution-based MS 10 min concentration-dependent activity assay. Control (red, square) and 1 μM SB-415286 (blue, circle). Data collected in MS2 mode.

Figure 2.8. Z' analysis of the GSK-3β solution-based MS assay with direct injection (top) or autosampler (bottom). +GSK-3β control reactions (circle), -GSK-3β control reactions (square), averages (blue) and 3 standard deviations (red).

Figure 2.9. IC_{50} curves for GSK-3β kinase activity collected over a 1 x 10^{-3} to 100 μM concentration range of SB-415286 (top) and GSK-3β Inhibitor II (bottom) and over a 0.1 to 200 μM concentration range of GSK-3β Inhibitor I (middle). 62.5 μM GSM, 125 or 25 μM ATP and 52.5 nM GSK-3β were incubated in 6 mM NH_4OAc/1.6 mM MgOAc, pH 7.4 buffer for 1 h. Control (125 μM) ATP concentration – blue, (●), decreased (25 μM)

ATP concentration – red, (■). Data is plotted after P/S values were added to the Hill equation on a log scale and normalized to the control values of the uninhibited reactions.

Figure 2.10. Preliminary solution-based ESI-MS analysis of a 100 compound inhibitor mixture in a screen for GSK-3β inhibitors. Black – pGSM/GSM ratio, pink – SB-415286 MRM signal trace (panels A & C). All signals averaged over their respective 6 min periods (panels B & D). Low control, high control, Mixture 1 – 10 (panels A & B). Low control, high control, Compound 11, 12, 13, 14, 20, 15, 16, 17, 18, 19 (panels C & D) (See Table 2.3 for compound data).

Figure 3.1. Diagram of a FAC/MS assay. Following the void marker, weak binders elute quickly. Retention is greater for strong binders, resulting in longer elution time (Figure originally published in Slon-Usakiewicz, J.J. et al., 2005, *Drug Discov. Today*[7]).

Figure 3.2. GSK-3β sol-gel leaching analysis with ^{32}P-ATP radioassay. % substrate turnover (pGSM (μM)/total GSM in reaction (μM)) obtained from 20 min washes with 6 mM NH_4OAc/0.8 mM MgOAc, pH 7.4 buffer (top) and cumulative enzyme activity over the 2 h wash period (μM pGSM/μg GSK-3β normalized to enzyme activity in solution) (bottom).

Figure 3.3. Radio assay GSK-3β sol-gel leaching analysis with 1 M KCl high salt wash. % substrate turnover (pGSM (μM)/total GSM in reaction (μM)) obtained from 20 min washes with 6 mM NH_4OAc/0.8 mM MgOAc, pH 7.4 buffer (top) and cumulative enzyme activity over the 2 h wash period (μM pGSM/μg GSK-3β normalized to enzyme activity in solution) (bottom).

Figure 3.4. Normalized assessment of GSK-3β inhibitor non-specific retention within blank sol-gel columns. 10 μM 1-Azakenpaullone (red, 1), GSK-3β Inhibitor VIII (blue,

2), SB-415286 (pink, 3) and 1 μM fluorescein (green, 4), all dissolved in 6 mM NH_4OAc/0.8 mM MgOAc, pH 7.4 buffer were injected at 5 μL/min for 20 min.

Figure 3.5. Inhibitor binding assay with 500 nM fluorescein (blue, 1)/50 nM SB-415286 (red, 2) (top) and 500 nM fluorescein (blue, 1)/10 nM SB-415286 (red, 2) (bottom).

LIST OF ABBREVIATIONS

ADP – Adenosine Diphosphate

APC – Adenomatous Polyposis Coli

ALIS – Automated Ligand Identification System

APTES – 3-aminopropyltriethoxysilane

ATP – Adenosine Triphosphate

DGS – Diglyceryl Silane

ESI-MS – Electrospray Ionization Mass Spectrometry

FAC/MS – Frontal Affinity Chromatography Mass Spectrometry

FRET – Fluorescence Resonance Energy Transfer

GLS – N-3-triethoxysilylpropylgluconamide

GSK-3α/β – Glycogen Synthase Kinase-3α/β

GSM – Glycogen Synthase Muscle (kinase fragment)

IMAP – Immobilized Metal-Ion Affinity Partitioning

IMER – Immobilized Enzyme Reactor

LANCE – Lanthanide Chelate Excitation

MALDI-TOF/MS – Matrix-Assisted Laser-Desorption Ionization Time-Of-Flight Mass Spectrometry

MeOH – Methanol

MRM – Multiple Reaction Monitoring

PEG – Polyethylene Glycol

TEOS – Tetraethyl Orthosilicate

TMOS – Tetramethyl Orthosilicate

Chapter 1

Introduction

1.1 Glycogen Synthase Kinase-3

Glycogen synthase kinase-3 (GSK-3) plays an intricate role within the framework of mammalian cellular metabolism, and is involved in many metabolic regulatory pathways. GSK-3 is unusual in that it is normally active in cells and is primarily regulated through inhibition of its activity. It is also unusual in that it has a preference for primed substrates that have been previously phosphorylated by another kinase. Unregulated GSK-3 activity has been implicated as the possible cause of a plethora of disorders, including Type II diabetes and Alzheimer's disease, making the protein an attractive target for drug development. GSK-3 exists as two isoforms, GSK-3α (55000 Da) and GSK-3β (51000 Da), both of which have conserved functionality. Acting specifically on serine or threonine residues located 4 amino acids N-terminal to a pre-phosphorylated (primed) Ser/Thr (Fig. 1.1), GSK-3 is able to inhibit glycogen and protein synthesis as well as effectively regulate many metabolic and growth factor proteins.[1,2] Structural studies of GSK-3β have elucidated that Arg 96, Arg 180 and Lys 205 assist in binding to phosphorylated substrates, while Asp 181 and Arg 220 are catalytic amino acids.[3] Regulation of GSK-3β activity occurs via phosphorylation of the Ser 9 residue near the N-terminus, resulting in the deactivation of the enzyme (Fig. 1.2). Various mechanisms exist to modulate enzymatic activity, including insulin induced GSK-3 inhibition via protein kinase B (PKB) of the PtdIns(3,4,5)P_3 protein kinase pathway, which inactivates GSK-3β/α through N-terminal S9/S21 phosphorylation.

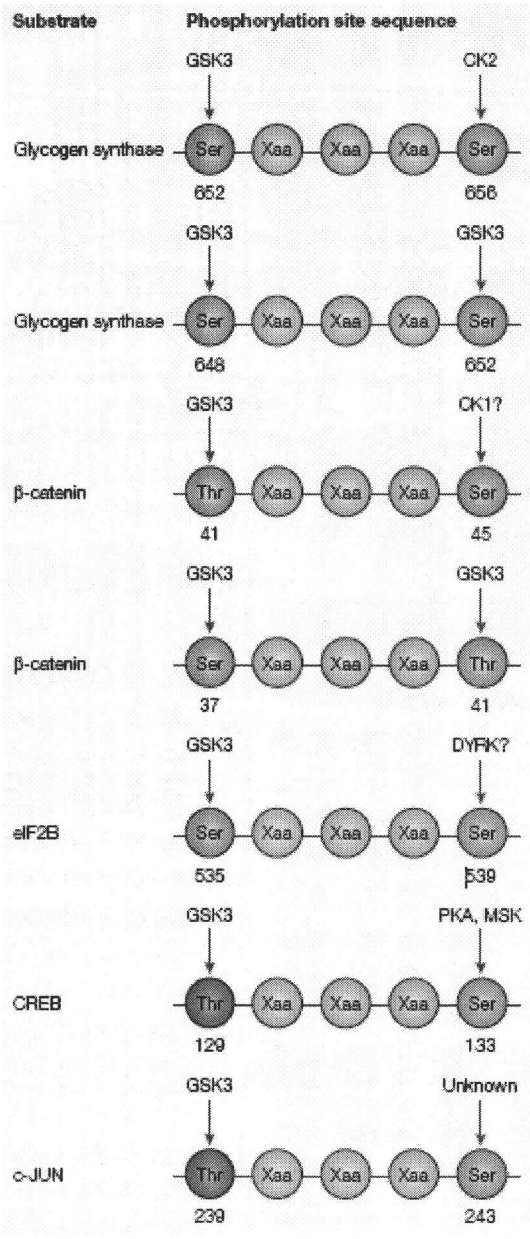

Figure 1.1: GSK-3 substrate phosphorylation is residue specific. GSK-3 phosphorylates target enzymes at Ser/Thr residues 4 amino acids N-terminal to the site of priming phosphorylation. CK2 – casein kinase 2, CK1- casein kinase 1, DYRK – dual tyrosine phosphorylated and regulated protein kinase, PKA – protein kinase A, MSK – mitogen and stress-activated protein kinase, eIF2B – eukaryotic protein synthesis initiation factor 2B, CREB – cyclic AMP-response element-binding protein (Figure originally published in Cohen, P. and Goedert, M., 2004, *Nat. Rev. Drug Discov.*[2]).

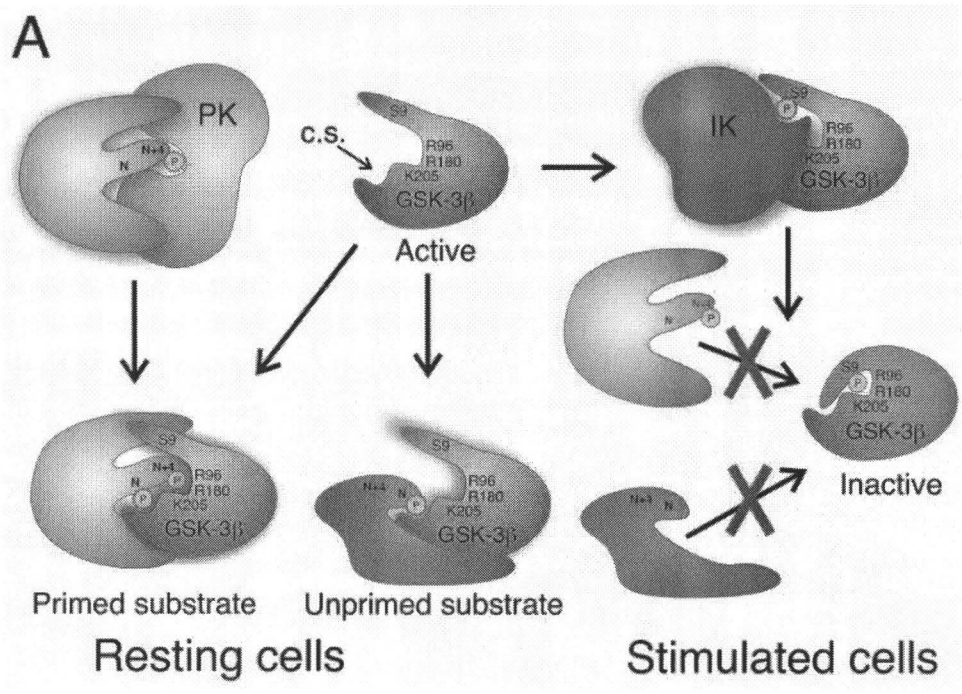

Figure 1.2: GSK-3β phosphorylates primed and unprimed substrates. Phosphorylation of S9 results in the blockage of the active site and kinase inhibition (Figure originally published in Doble, B.W. and Woodgett, J.R., 2003, *J. Cell Sci.*[1]).

Regulation of glucose metabolism is one of the chief roles of GSK-3. As a kinase, the enzyme achieves this goal through the inhibition of glycogen synthase (GS) via phosphorylation. Thus, during periods of low blood glucose concentration, characterized by the absence of insulin (an indirect inhibitor of GSK-3), glucose levels in the bloodstream are increased by inactivation of GS. However, once the glucose levels in the blood begin to rise, insulin initiates GSK-3 inhibition after binding to a specific cell surface receptor. The resulting autophosphorylation of the receptor propagates a signal through a chain of interdependent kinase shuttles via phosphate group transfer. Eventually, Ser 9 of GSK-3β is phosphorylated via this mechanism, relieving the inhibition of glycogen synthase and other proteins such as eIF2B, allowing glycogen and protein synthesis to proceed.[4,5]

Although GSK-3 has been proven as an efficient regulator of cellular metabolism, responsible for the modulation of several vital processes, deviations in its activity often prove catastrophic for the organism. The most frequent GSK-3 dysfunction involves the uncontrolled phosphorylation of its targets, resulting in manifestations of various diseases. The hyperphosphorylated targets of GSK-3 have been implicated in causing: A) Type II diabetes, via constant inhibition of glycogen synthase (sugar storage mechanism), resulting in elevated levels of blood glucose for prolonged periods of time; and B) Alzheimer's Disease, via hyperphosphorylation of the filament producing protein Tau, leading to aggregation and plaque formation in neurons, causative agents of cell death.[4]

While inhibition of the enzyme appears to be an obvious therapeutic route to overcome the negative role of GSK-3β in the development of the diseases noted above, the inhibition of the enzyme could presumably lead to enhanced accumulation of unphosphorylated β-catenin, a known oncogene activator.[1] Under normal circumstances, the phosphorylation of the casein kinase I (CKI)-primed β-catenin by axin-associated GSK-3 leads to its proteasomal degradation post ubiquitylation. However, should the active site of GSK-3 be blocked, β-catenin will remain unphosphorylated and will then translocate to the nucleus, activating T-cell factor/lymphoid enhanced factor (TCF/LEF) proteins which stimulate the transcription of oncogenic genes, leading to cancer.[6,7,8] Therefore, it is of vital importance to discover compounds that will selectively prevent excessive glycogen synthase and tau phosphorylation via blockage of the special primed substrate binding sites, while simultaneously leaving the β-catenin pathways unaltered. This will require the inhibition of only the glycogen synthase/tau binding sites without blocking either the ATP binding active site or the axin binding site (Fig 1.3).

Although steps have been take to counter the effects of GSK-3 dysfunction, the majority of the available kinase inhibitors that have been identified all suffer from the same fundamental drawback – they inhibit ATP binding to the active site. This effect is undesirable from the point of view that it leads to the cessation of phosphorylation of all GSK-3 targets, including β-catenin. Potential also exists for "off-target" inhibition of ATP binding sites of other kinases with active sites constituted of similar amino acid sequences. To identify compounds that selectively block the glycogen synthase/tau binding sites while retaining the ability to bind ATP, a screening technique with the capacity to extract these inhibitors is required. The use of mass spectrometric assay techniques to assess turnover of primed substrates may be able to achieve this goal, and when utilized with varying ATP or glycogen synthase/tau concentrations, should also be able to assess site of action. Such an assay could also be adapted to the solid phase via GSK-3β immobilization, and used as an affinity-based screening tool to identify and isolate bioactive compounds from organic compound libraries or natural product extracts that can consequently be applied toward the development of effective treatments for GSK-3 related diseases. Development of such assays is a key goal of this thesis project.

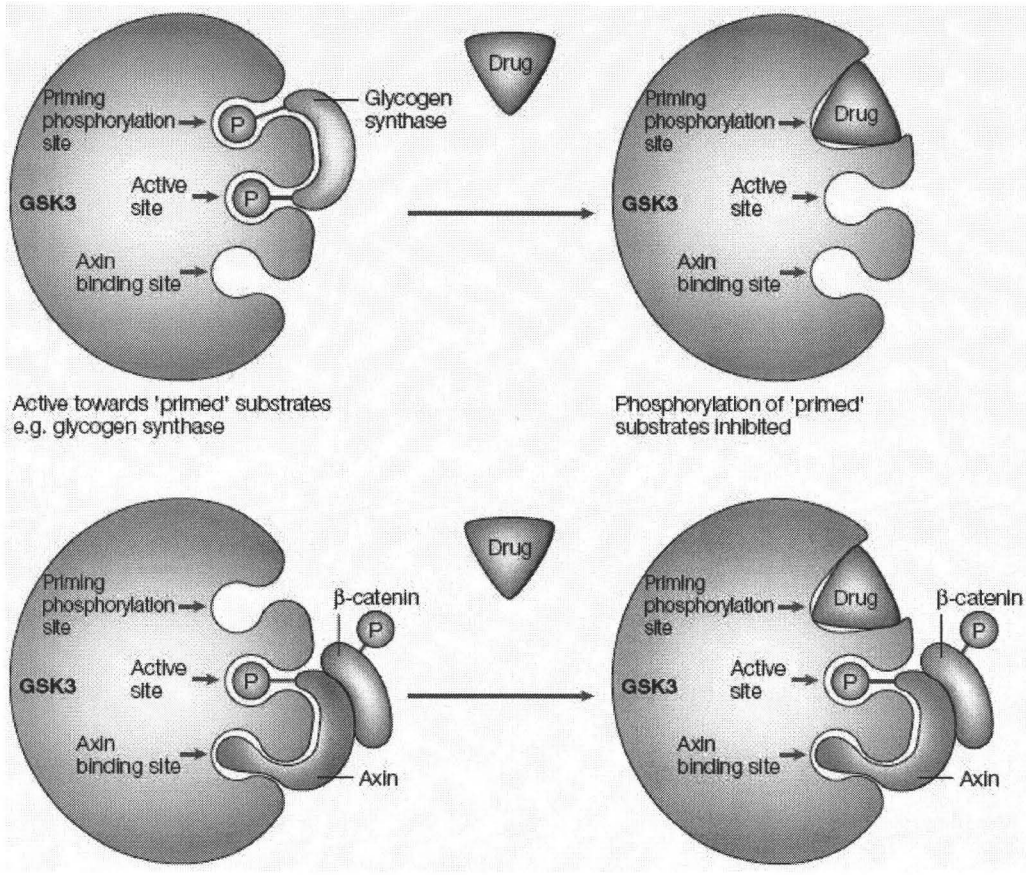

Figure 1.3: Medically relevant drug development for GSK-3 disorders must be selective in deactivating only the priming phosphorylation site - the binding site of glycogen synthase. Inhibition of the active site is undesirable, as it can deregulate cellular processes (Figure originally published in Cohen, P. and Frame, S., 2001, *Nat. Rev. Mol. Cell Biol.*[4]).

1.2 Kinase Inhibitor Screening

Table 1.1 contains a broad sample of typical assays that are currently employed academically and industrially in the screening of kinase inhibitors. The methodologies behind these systems as well as their effectiveness for high-throughput screening of GSK-3 inhibitors are discussed in the following sections.

Method	Mode of action	Procedure/Detection	Major disadvantage
Cell based assays[9]	Change in cell phenotype	Utilize specific antibodies to obtain chemiluminescent signal via ELISA.	Requires extensive development of protein specific antibodies.
Luciferase assay[10]	ATP to ADP conversion	Luciferase signal proportional to ATP concentration.	High ATP sensitivity of luciferase.
Coupled reaction assay[11]	ATP to ADP conversion	ADP oxidizes NADH – 340 nm absorbance decreases.	Secondary proteins could be affected by inhibitor.
LANCE assay[12]	Tyr to pTyr conversion	Tyr phosphorylation brings Eu to fluorophore – emits light at 665 nm.	Can't discern between multiply phosphorylated substrates.
^{32}P radio assay[14]	Tyr to pTyr conversion	pTyr product ^{32}P labeled during incubation – count radioactivity.	Slow – need to count radioactivity.
Pro-Q assay[15]	Tyr to pTyr conversion	Binds to phosphorylated proteins selectively – emits light at 580 nm.	Can't discern between multiply phosphorylated substrates.
TruLight technology[18]	Fluorescence quenching	Utilizes a superquenching substrate technology.	Can't work with primed substrates.
Iron Quenching[19]	Fluorescence quenching	Iron chelant binds to phosphorylation site, quenches fluorescent peptide.	Needs labeled substrate, may not work for most classes of kinases.
IMAP[20]	Fluorescence polarization	Uses nanoparticles for detection.	Requires use of FP or TR/FRET – potential for fluorescence interference
FP methods[21]	Fluorescence polarization	Displace fluorescent analog of an inhibitor, decreasing polarization.	No direct indication of functional inhibition, need labeled substrate, hard to use with fluorescent inhibitors.
ALIS[22]	Affinity screening	Use SEC to separate bound and free ligands. Detect displaced inhibitors by MS.	No information about where the inhibitor binds or if it affects function.
FAC/MS[27]	Affinity screening	Target covalently immobilized – monitor inhibitor retention by MS.	No information about where the inhibitor binds or if it affects function.
BioTrove HTS[31]	Enzyme reactor/MS	Incubate inhibitor with protein – monitor product with MS.	Expensive to replace protein for each assay.
Reaction Loop/MS[32]	Affinity screening/ER	Inhibitors affinity separated, then react with protein – monitor product with MS.	Expensive to replace protein for each assay.
Silica column/RPLC[33]	IMER	2D IMER/RPLC with UV-Vis detection.	Screen is slow due to RPLC step.
Silica column/MS/MS[36]	IMER	Continuous flow IMER with ESI-MS detection.	Must use low ionic strength buffers.

Table 1.1: Current kinase inhibitor screening technologies.

1.2.1 *In Vivo* Assays

1.2.1.1 Change in Cell Phenotype

Among the plethora of cell-based kinase assays currently available, fast activated cell-based ELISA (FACE) is one of the methods specially tailored toward high-throughput screening, relying on a colorimetric or chemiluminescent readout to indicate phosphorylation.[9] Although this technology allows the inhibitors to interact with their substrate in a natural cell environment, it is difficult to discern whether the target kinase is inhibited by the compound directly or whether it is acting on another component of the pathway. These assays also require the extended and costly development of protein-specific antibodies, which greatly narrows down the range of kinases that can be assessed with this method.

1.2.2 *In Vitro* Assays

Although there is a large selection of *in vitro* assays available on the market for kinase inhibitor screening, the majority of them are based on the principle of accurately monitoring enzyme functionality through secondary reporter molecules. Some of these methods focus on either the detection of ADP (Luciferase) [10,11] or the quantity of the singly phosphorylated product formed during a reaction (LANCE, Pro-Q)[12,13], but require coupled enzyme/antibody reactions to produce signal. Other assays, such as those that rely on the measurement of fluorescence polarization, are based on the change in probe polarization as a factor of substrate conversion, but require labeled substrate (competitive FP assay)[20,21]. Conversely, affinity technologies do not measure activity directly, but instead can rank potential inhibitors in order of their affinity for the protein. This method

does not, however, disclose an inhibitor's site of binding or its effect on activity (FAC/MS)[22,27]. Despite their individual versatility, the collective suitability of these methods for monitoring GSK-3 activity is poor, due to the specific nature of the enzyme's mono-phosphorylated substrate and multi-phosphorylated product. As many of these kinase assays are geared toward discrimination between a non-phosphorylated substrate and a mono-phosphorylated product, they can not discern between the unusual substrate/product of GSK-3β. A brief summary with more in-depth explanations of specific representatives of each category is provided below.

1.2.2.1 ATP → ADP Conversion

The Kinase-Glo Luminescent Kinase Assay is a luciferase based approach which measures enzyme activity by oxidizing luciferin using ATP to produce light.[10] A major obstacle for efficient high-throughput screening inherent to this system is the high sensitivity of luciferase to ATP, which limits the concentrations of ATP in the assay (20 μM vs. ~1 mM) and may significantly bias the screen in favour of ATP-competitive inhibitors.

Coupled reaction assays involving colorimetric/fluorimetric compounds, such as the phosphotransferase assay, are a commonly used tool in inhibitor screening. Through a sequence of coupled protein reactions designed to oxidize NADH, this method monitors the drop in absorbance of NADH, which correlates with the production of ADP.[11] While this approach is amenable to the screening of inhibitors on an individual basis, a possible problem could arise if the inhibitor in question affected a secondary protein instead of the

intended target kinase. Specific control experiments for every inhibitor would be required, as the results of such assays may be potentially misleading.

1.2.2.2 Tyr → pTyr Conversion

An example of technology involving fluorescent labeling to detect kinase activity, is the homogeneous time-resolved fluorescence energy transfer assay (LANCE), based on the detection of a fluorescence signal created by a product-specific anti-pTyr antibody.[12,13] Although this technique can indicate the successful phosphorylation of an unphosphorylated substrate and can detect competitive inhibitors via reduced FRET, a primed substrate will inherently elicit a signal prior to its phosphorylation by the kinase. Also, as phosphorylation often occurs at both Thr and Ser sites, anti-pTyr antibodies will not work with all kinases.

Conventional radio-labeling assays require ^{32}P isotopes for kinase studies, and are able to directly report on the phosphorylation of a substrate by measuring incorporated radioactivity counts after washing away free ^{32}P label. While this assay is amenable to reactions involving multiply phosphorylated substrates such as those that are targeted by GSK-3β, certain aspects of this methodology provide substantial drawbacks for successful inhibitor screening.[14] For example, radio assays require significant periods of time to provide a result, require special handling and safety protocols and are not easily adapted to screening of mixtures.

Another pTyr/Ser/Thr assay involves staining of reaction products with the Pro-Q Diamond phosphoprotein stain followed by analysis of emission intensity in the solid-phase.[15,16,17] A key issue with this method is the high background that is inherent with the

use of a primed substrate, as the stain was initially developed for assays involving non-phosphorylated substrates. Thus, an increase in emission intensity caused by phosphorylation of a primed substrate may be difficult to quantify.

1.2.2.3 Fluorescence Quenching

The TruLight Kinase Assay is an example of screening technology that depends on the detection of fluorescence quenching at one wavelength and emission at another, proportionally correlated to substrate phosphorylation. Metal ions coordinate phosphorylated peptides labeled with quencher to fluorescent polymers, resulting in increased emission at 600 nm in the presence of enzyme activity.[18] As this technique is primarily intended for unphosphorylated substrates, application to GSK-3 inhibitor screening is not possible due to its inherent inability to distinguish between a single phosphate on a product and a single phosphate on a substrate.

The iron quenching assay is a similar method, where phosphorylation of the substrate is detected by a drop in fluorescence intensity that occurs after the reaction of a metal-containing compound with the product.[19] Again, the key obstacle is the inability to discriminate between a primed substrate and a product with one phosphate. This method also requires the labeling of substrates with a fluorophore, which prevents the use of natural substrates.

1.2.2.4 Fluorescence Polarization

The Immobilized Metal-ion Affinity Partitioning (IMAP) assay monitors the change in the fluorescence polarization of a fluorescently labeled peptide/protein, with increased

fluorescence polarization observed following its phosphorylation due to the binding of a metal ion.[20] Although this method may be utilized for high-throughput screening, as it is resistant to fluorescence interference due to the high concentration of fluorophore used, it is not amenable for use with GSK-3, as it would exhibit similar polarization for the substrate and product.

A competitive fluorescence polarization (FP) assay for kinases involves the displacement of a fluorescent phosphorylated peptide from an anti-phospho-serine antibody by the kinase reaction product, leading to a drop in the polarization signal.[21] Its relative simplicity aside, certain aspects of this technique prevent it from being useful in high-throughput screening: first, is the inability to process primed substrates; and second, is the potential for fluorescence interference if fluorescent inhibitors are used.

Despite their wide applicability to conventional kinase research, the aforementioned screening methods fail to properly address the issue of phosphorylated substrate/product discrimination, as they largely rely on a binary mode of activity detection. To properly tackle this issue, another methodology was needed, namely that of mass spectrometry (MS) – a system applicable to GSK-3β research due to its intrinsic capacity to discern between phosphorylated substrates/products by mass alone.

1.2.2.5 Affinity Screening

Affinity based screening methods are often used to identify ligands that bind to target proteins. They can be implemented in several formats and used to screen both discrete compounds and mixtures. All affinity-based methods have in common the need to separate the protein-ligand complex from free ligands present in mixtures. Variants of

affinity methods include solution-based assays that utilize size exclusion chromatography or pulsed ultrafiltration to separate complexes from free ligands, and solid-phase assays where the target protein is immobilized in a column and used to identify compounds on the basis of retention on the column.

An example of a solution-based affinity screening method is the Automated Ligand Identification System (ALIS), which is an affinity-based size exclusion chromatography/mass spectrometry (SEC-MS) technique. By increasing the concentration of a known competitor compound, ligand binding affinity to a protein can be ranked, thus separating potent and weak inhibitors.[22] Other affinity related methods such as size-exclusion chromatography[23,24], pulsed ultrafiltration[25] and affinity capillary electrophoresis[26] suffer from the same drawbacks as ALIS in that they do not reveal the inhibitor's site of action nor its effect on enzyme activity and kinetics, but they can screen mixtures, provided a specific inhibitor is available as a marker for competitive displacement chromatography.

An example of a solid-phase assay is frontal affinity chromatography coupled with MS-based detection (FAC/MS), which has been widely applied for screening mixtures.[27] This method usually involves covalent or affinity-based immobilization of the target protein to a solid support structure (normally silica), followed by pumping of the analytes in the mobile phase through the column. Each inhibitor compound establishes an equilibrium with the enzyme binding site, resulting in a specific elution gradient, where the weak binding compounds exit the column first.[28,29,30] This method does not directly assay the protein in the presence of substrate, and thus cannot provide information on the extent of activity suppression by a given compound. Also, denaturation and deactivation

of target protein can occur upon immobilization and non-specific binding of compounds to the column support material can lead to false positives which must be controlled for by using blank control columns.

1.2.2.6 MS Analysis of Enzymatic Reactions (ER/MS) in Solution

The RapidFire XC-MS System is a method that uses tandem mass spectrometry to follow the conversion of a substrate to a product in solution, with the simultaneous direct monitoring of their concentrations.[31] While a typical automated p450 solution inhibitor assay in this format is run at 8-10 s/sample, demonstrating the screening speed of a mass spectrometer, the processing of the samples requires a chromatographic purification step prior to MS injection, increasing the individual sample processing time. The non-reusability of the target protein is also a disadvantage, as it is not cost-effective to replace protein for every new assay.

Yet another method for following enzymatic reactions by MS is to use a "continuous flow reaction loop" in which the enzymatic reaction occurs interfaced directly to a MS to monitor substrate turnover. As in a solution-phase assay, the enzyme is continuously infused into the MS along with substrate.[32] While this is a useful method for functional mixture screening, the continuous infusion of protein into the MS can prove costly for some assays.

Although effective at detecting the presence of numerous ligands in real-time, Electrospray Ionization-Mass Spectrometry (ESI-MS) technology has a significant limitation that should be taken into consideration when dealing with mixture screening. The presence of readily ionized compounds, such as metal ion salts and organic

molecules like DMSO, poses a problem to the detection sensitivity of the method. As a result of high charge absorption, these compounds are rapidly ionized in the MS, preventing the further ionization of the desired sample molecules. Consequently, optimization to determine the ideal ionic strength for the reaction that is mutually compatible with protein activity and MS detection is required.

1.2.2.7 Immobilized Enzyme Reactor (IMER) Methods

There are a large number of IMER-based screening assays in the literature, although the exact implementation of the IMER for screening varies. Most groups infuse a plug of substrate along with a single inhibitor into an IMER with a second dimension of chromatography to separate the product and substrate with absorbance or MS based detection to assess the amount of product formed.[33] While these IMER methods are capable of carrying out typical Michaelis-Menten kinetic studies, two major drawbacks prevent it from performing effective high-throughput screening. First, the need for a post-IMER RPLC separation step to purify the sample prior to MS infusion can significantly increase the time required to complete the assay. Furthermore, this prevents effective screening of compound mixtures, as it is not easy to deconvolute the mixture to identify potent compounds.[34]

An alternative IMER method has been described wherein the IMER (with no RPLC) was directly interfaced to a tandem mass spectrometer with the infusion of plugs of substrate (with or without an inhibitor present), permitting both Michaelis-Menten and inhibition studies to be done. However, mixture screening was not demonstrated in the study. A potential drawback of this method is the direct interfacing of the MS system to

the column, which restricts the use of buffers with high ionic strength owing to their propensity to cause ion suppression.[35]

Previous work within the Brennan lab group has laid the foundations for a practical screening technology that combines IMER/MS with the continuous flow enzyme reactor loop method. Specifically, a substrate is continuously infused through a sol-gel column containing an immobilized enzyme and the product/substrate ratio is continuously monitored by tandem MS. As the substrate is infused through the column, it is partially converted to product. Both substrate and product are detected using an (ESI-MS) system.[36,37] Inclusion of an inhibitor results in alteration of the product/substrate ratio in favour of substrate, providing a functional screening method. This approach has the demonstrated advantage of being amenable to screening and deconvolution of simple mixtures, and can be partially automated by using an autosampler to introduce different compound mixtures to the column. As well, the inhibitor has the opportunity to reach equilibrium with the bound protein, which is not true for the case of plug injection. Another advantage is the same column used for IMER/MS can be used for follow-up FAC/MS studies by removing the substrate from the assay. Finally, the continuous flow method inherently leads to bioselective solid-phase microextraction (bioSPME) of any potent inhibitors bound to the protein. This process entails the use of sequential washing to remove weak and then strongly bound ligands for direct analysis by MS and has the potential for rapid identification of strong inhibitors from complex mixtures following functional IMER screening.[38]

1.3 MS Based Kinase Characterization and Inhibitor Screening

With the need for improved efficiency in kinase inhibitor screening and hit detection becoming more apparent in the constantly expanding field of drug development, a versatile and robust approach such as electrospray mass spectrometry has the demonstrated potential to become an indispensable high-throughput screening technique. As with any MS technology, the basic premise of ESI-MS/MS is the detection of compounds by mass alone, subsequently rendering obsolete any secondary labels commonly required in other kinase screening methods. Upon entering the mass spectrometer, the liquid analyte is passed through a fine tipped metallic needle with a charge of -4500 V, which results in the nebulization and ionization of the mobile phase. These compounds (known as parent ions at this stage) will usually form adducts with H^+ ions, proportionally to the quantity of positive charges present on the molecule. Through the application of RF fields, quadrupole 1 (Q1) is responsible for the mass filtration of the molecules, based on the settings defined in the software. A high and a low mass limit is therefore created to allow the passage of only the desired parent ions. These selected compounds then proceed into quadrupole 2 (Q2) where N_2 gas particles entering the mass spectrometer can be used to break up the molecules into smaller compounds via collision induced dissociation. This process is the result of intense kinetic energy transfers from the incoming N_2 particles to the parent ions, resulting in molecular bond fractures at the points of least stability. Newly produced daughter ions are imbued with a positive charge and undergo H^+ adduct formation. These parent and daughter ion adducts (MH^+) will enter quadrupole 3 (Q3) where RF fields will again select only the required parent ion/daughter ion pairs, allowing them to reach the detector. The ions picked up by the

detector will be converted into electrical signals by the electron multiplier and translated by the software into interpretable data as a mass to charge ratio.[39] Thus, the key advantage of ESI-MS/MS is the capacity for the precise selection of specific compounds, owing to the unique daughter ions formed in Q2. This allows exclusive monitoring of the desired ion pairs without signal interference, or noise,
originating from other molecules and their fragments. The main disadvantage of this method is its sensitivity to the presence of salts and other easily ionized compounds, which decrease the capacity for ligand ionization, negatively affecting signal intensity through the creation of unnecessary adducts.

Electrospray mass spectrometry has been utilized by our group previously in IMER/MS studies involving the conjunction of monolithic protein-doped sol-gel columns with ESI-MS/MS detection. The ubiquitous metabolic enzyme adenosine deaminase (ADA) utilized in those experiments, performs the water catalyzed conversion of adenosine to inosine via the hydrolysis of the purine amine group to a hydroxyl group.[40] Columns containing entrapped ADA were able to turnover adenosine to inosine, and direct interfacing of the columns to a tandem MS system was shown to be viable for quantitative detection of product formed on-column (Fig. 1.4). The known competitive inhibitor erythro-9-(2-hydroxy-3-nonyl) adenine (EHNA) was used as a model inhibitor for a miniaturized small molecule screen. Through the addition of an autosampler unit, a set of 7 mixtures of 7 compounds each was introduced into the column sequentially.[36] A sharp decrease in the inosine signal was recorded upon infusion of the mixture containing compounds 36-42, while assaying of individual compounds in this mixture confirmed that EHNA was indeed responsible for ADA inhibition. While this proof-of-concept test

is by no means a high-throughput assay, it points to the potential of this method for high-throughput compound screening for other enzymes. Experiments performed on sol-gel entrapped nicotinic acetylcholine receptor (nAChR) involving FAC-MS, demonstrated another useful application of mass spectrometry. Through the addition of 200 nM fluorescein (void marker) and 25 nM epibatidine (a strong nAChR binder), the difference in elution time between the two compounds (~3 min vs. ~27 min) revealed that receptor was able to retain its active conformation within the silica column.[41] Further exploration of FAC/MS to study concentration dependent changes in the elution of epibatidine yielded B_t (amount of protein immobilized) and K_d (dissociation constant) at close to literature values (1.6 pmol and 3.4 nM), proving that 100% of the initially loaded protein remained active in the sol-gel matrix. This demonstrates the potential of the sol-gel/MS-based method for mixture screening, as it would allow for sol-gel entrapped enzyme reusability in IMER/MS and FAC/MS assays.

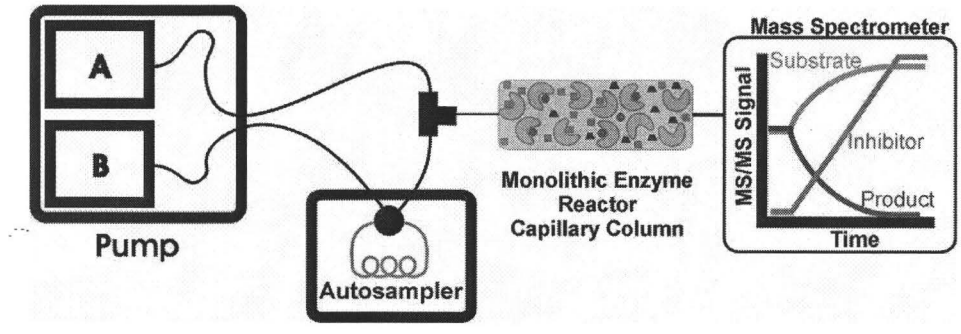

Figure 1.4: Sol-gel based method for inhibitor screening using IMER/MS technology. All mobile phases and samples contain an identical concentration of substrate, while inhibitors are 1) introduced by pump B, either through loading directly into reservoir of pump B (top) or 2) through an autosampler loop (bottom). The sol-gel column immobilizes the enzyme, allowing for interaction with multiple inhibitors. The effect of the inhibitors on substrate/product signal is monitored via ESI-MS. The first method is designed for quantitative analysis of identified inhibitors, while the second method is utilized for automated screening of multi-compound mixtures (Figure originally published in Hodgson, R.J. *et al.*, 2005, *Anal. Chem.*[36]).

Other incarnations of MS technology, such as matrix-assisted laser-desorption ionization time-of-flight mass spectrometry (MALDI-TOF/MS) have also been successfully applied toward inhibitor screening for numerous proteins. Unlike ESI-MS, MALDI relies on laser induced, instead of charge induced, ionization of compounds, resulting in [MH^+] adduct formation.[42] Molecules usually acquire only one charge and can be found at a mass to charge ratio corresponding to their molar mass. This method has fewer restrictions on the concentration of buffer/salts used and possesses a high mass detection limit, permitting ionization of proteins as large as 2 MDa.[43] For example, the particular type of MALDI performed by the Mrksich group involves self-assembled monolayers or SAMs, which are composed of a gold covered glass plate with substrates/ inhibitors/co-factors deposited in an array into grooves on its surface. The enzyme is then printed onto these grooves and the reactions are allowed to proceed for a set period of time. Once the incubation is completed, the contents of these grooves are ionized by a pulsed laser and the signals are analyzed by TOF/MS. This method has been used to screen for inhibitors of anthrax lethal factor and monitor activity of arginine methyltransferase 1 (RMT1) and c-Src kinase.[44,45,46]

While the studies outlined above have established the potential of mass spectrometry as a promising and versatile technology for mixture screening, the suitability of this method for GSK-3 remains to be demonstrated. However, there are a number of advantages inherent to MS technology that make it ideal for GSK-3 studies. 1) ESI-MS/MS can easily discriminate primed substrates from multiply phosphorylated products and thus directly monitor kinase activity. 2) Furthermore, this technique has the ability to discriminate between inhibitors that bind the ATP site and those that bind the primed

substrate binding site by varying of ATP and primed substrate concentrations during IMER/MS analysis. 3) Continuous flow IMER/MS can also potentially be scaled up to operate effectively at high-throughput levels due to its capacity to reuse the immobilized target protein. 4) The ability to handle either discrete molecules or mixtures is conducive to the screening of increasingly complex sets of drug-like compounds or of natural product extracts. 5) This system should provide an excellent opportunity for the evaluation of combined IMER/MS and affinity chromatography screening modes for the deconvolution of complex mixtures. While such advantages make the use of IMER/MS attractive, a significant number of issues remains to be overcome to make the method amenable to GSK-3 screening: 1) Potential problems arising from loss of activity or poor accessibility of entrapped GSK-3β; 2) calibration and detection sensitivity for substrates, products and inhibitors affected by poor ESI-MS/MS detection in the presence of salts and buffers due to charge stealing; 3) non-specific binding of substrates or inhibitors to the column, resulting in the inability to accurately determine the amount of substrate and product; 4) problems assessing the site of action of inhibitors; 5) absence of optimization for operation with complex mixtures, and hit deconvolution. Addressing these issues forms the basis of future research and development in the field of continuous flow IMER/MS. As the studies outlined above have established the potential of IMER/MS as a powerful new method for mixture screening, the application of this approach against kinases such as GSK-3 will definitively verify its versatility. Mass spectrometry holds much promise for an enzyme like GSK-3, participating as a crucial step toward medically relevant drug development.

1.4 Sol-gel Bioimmobilization

Since 1990, when the Avnir group reported the first retention of a protein in a biochemically active, tetramethyl orthosilicate (TMOS) derived sol-gel glass, protein entrapment in silica has become a rapidly developing field, merging with existing methods in analytical chemistry, biochemistry and chemical genetics.[47] Numerous studies have been published since then, with most focusing on immobilized protein characterization. The Zusman group's work, for example, focused primarily on the entrapment of antibodies with gel fiberglass (GFG) membranes used for support, applied for screening of tumor-associated antigens (TAA) from the blood of cancer patients.[48] Toyo'oka's group performed a series of experiments with sol-gel immobilized proteins on chips and in columns separated electrophoretically using capillary electrochromatography.[49,50,51]

Due to its potential for protein reuse in inhibitor screening, enzyme entrapment in cross-linked silica polymers features prominently in our group's research as well. One such silicon-based precursor is diglyceryl silane (DGS). Derived from the reaction of TMOS and glycerol, it is frequently used in sol-gel synthesis as a structural ingredient.[52] In the presence of H_2O, DGS is hydrolyzed, releasing glycerol and allowing the remaining silica structures to cross-link and solidify. This results in a SiO_2 polymer matrix permeated with very small pores (mesopores) with an average diameter of 3.6 nm. The inclusion of the porogen polyethylene glycol (PEG) to the sol-gel reaction produces large pores in the matrix at ~0.5 μm in diameter (macropores) as a consequence of spinodal decomposition. Phase separation of the silica and PEG from H_2O then occurs, leaving a hardened silica structure with PEG and glycerol inside. Proteins dissolved in

buffer can also be added to the reaction and will become entrapped inside the mesopores, with the silica chains molding a shape-specific cavity around them.[53] As a side effect of using DGS, the presence of glycerol helps the stabilization of the proteins and prevents the loss of activity that can occur from using other silica-derived precursors.

The primary purpose of the mesopores is to retain the protein, while the macropores regulate the flow of solution through the sol-gel. Correct proportions in a protein-doped sol-gel usually include ~50% mesopore volume and ~23% macropore volume. With too few macropores, the backpressure in the column would be too high due to flow problems, while too many macropores would cause excessive enzyme leaching. Certain factors have been demonstrated to affect this ratio and a thorough understanding of the effect the reagents have on the sol-gel process is important. One of the key aspects affecting both the porosity and polymer interaction is the pH of the buffer used in the making of the sol-gel, which is optimal at 7.0 – 7.4 when manufacturing from DGS. Increasing the pH above this value results in shorter coarsening time, causing faster gelation and a high percentage of mesopores to macropores owing to the formation of the gel network before most of the phase separation occurs. This is not usually desirable, as highly mesoporous sol-gels will not easily allow flow through a column and can cause serious pressure driven fracturing of the silica. Conversely, dropping the pH below 7 will cause longer coarsening time, which will create a high number of macropores, allowing total leaching of enzyme to take place. Another method of manipulating porosity requires changing the percentage of PEG in the solution, as it regulates gelation and phase separation processes via its interaction with the silica surface. With 5% PEG being the standard for sol-gel synthesis, dropping the amount of PEG to 2.5% has been shown to decrease the gelation

time and increase the mesoporosity. This is caused by a higher concentration of silica particles relative to the PEG, which leads to faster condensation and polymerization, creating smaller pores. At 5% PEG, enough of the polymer envelops the silica strands to diminish the interaction between them, increasing the gelation time and the amount of macropores. Raising the PEG concentration above 5% will cause a small increase in the gelation time, but will not affect the overall procedure significantly, highlighting pH as the primary means of control over the characteristics of a sol-gel.[37]

A study performed by our group aimed to examine the effects of column morphology and flow rates on the kinetic parameters of an entrapped enzyme in a sol-gel column. A key issue with enzyme assays is the need to work with substrate conversion levels below 10% so that initial reaction rates remain proportional to product concentrations. While previous IMER studies using plugs of substrate have shown that immobilized enzymes can provide reliable kinetic parameters, such studies had not been performed under conditions of continuous flow. Using columns containing entrapped γ-glutamyl peptidase (γ-GT), the conversion of L-glutamic acid *p*-nitroanilide (GPN) to *p*-nitroaniline was determined as a function of substrate concentration at different flowrates. Although the kinetic data for the γ-GT protein was shown to follow the Michaelis-Menten equation, indicative of normal protein function, it became clear that the kinetic parameters were dependent on the flowrate, which is in fact a manifestation of the effects of increased backpressure. As backpressure rose (at high flow rates and low porosity), the substrate was able to diffuse more rapidly to the enzyme active site, leading to an increase in k_{cat} values with the K_m simultaneously dropping, most likely due to more efficient transport of substrate to the entrapped enzyme. As well, increased sol-gel porosity with higher

macropore volume at lower pH, was demonstrated to cause more leaching and lower backpressure, automatically limiting substrate conversion. A low product concentration permits to accurate monitoring of changes in activity, and validates the applicability of sol-gels to the determination of enzyme kinetics.[37]

1.5 Goals of this Thesis

1.5.1 Solution-based ESI-MS GSK-3β Inhibitor Screening

Although a multitude of kinase assays capable of verifying enzyme activity currently exists, none are particularly well suited for detecting GSK-3 substrate conversion. The primary cause of this problem is the inherent limitation of these methods that allows them to only discriminate between an unphosphorylated substrate and a singly phosphorylated product. Since GSK-3 acts on a mono-phosphorylated substrate and creates a multi-phosphorylated product, the background signal generated by the substrate in these assays would be nearly indistinguishable from that of the product, preventing any inhibitor screening from taking place. The primary goal of this thesis stemmed from these issues, and is as follows: to develop a technique that would discern in a simple and rapid fashion a di-phosphorylated product from a mono-phosphorylated substrate in order to both effectively monitor GSK-3β activity and to allow high-throughput screening to take place. As MS technology has already proven to be a powerful tool in enzyme studies, especially in the area of proteomics, its benefits to GSK-3 research became apparent. In particular, the ability of a mass spectrometer to distinguish between molecules based on mass alone, has the great advantage of simultaneously monitoring both the substrate and the product. After establishing a solution-based ESI-MS/MS compatible assay format, the

procedure was verified by ^{32}P radio assays, the only other currently existing non-MS means of properly detecting GSK-3β activity. The method was subsequently validated for high-throughput screening with a Z' value acquired by performing a statistical reproducibility test, designed to assess the level of consistency of an assay by determining the statistical average and standard deviation for the activity induced by (±) GSK-3β controls. The accuracy of this technique in monitoring enzyme inhibition was then evaluated by generating IC_{50} curves with known GSK-3β inhibitors added. Through the variation of ATP and GSM concentrations, these studies also provided information on the site of action of these inhibitors, confirming the applicability of this method for confirmation of hits in secondary screening. Further development of the solution-based ESI-MS/MS assay focused on the primary screening of inhibitors from synthetic compound libraries utilizing semi-automated mixture screening via the nanoLC/MS/MS system.

1.5.2 GSK-3β Sol-gel Immobilization

As demonstrated by numerous examples in the literature, the application of sol-gel immobilized enzymes in characterization and inhibition studies is a promising and expanding field with great potential for future applications. The specific advantages of sol-gel entrapment over traditional immobilization methods include prolonged protein stability, reusability for multiple assays and retention of native conformation due to the absence of covalent binding to the solid phase. In particular, the entrapment of kinases in silica derived sol-gel has already been shown to yield useful data such as IC_{50} curves for existing inhibitors, with enzymes including Src kinase, protein kinase A and creatine

kinase. With the obvious advantages of this approach evident, we sought to extend this methodology to GSK-3β, focusing on the potential for immobilization of this protein within sol-gel materials. First, we performed leaching studies by utilizing ^{32}P radio assays, with sol-gel monoliths containing GSK-3β, testing for enzyme loss after exposure to continuous washes. This was followed by assessment of the utility of sol-gel columns for affinity based inhibitor screening and not IMER/MS, as the negatively charged silica surface would require surface modification to prevent positively charged substrate/product molecules from binding. Since affinity screens rely solely on the strength of compound interactions with the protein, the system was first tested with established ATP-competitive inhibitors. To account for possible unfavourable inhibitor interactions, non-specific binding to the silica was first examined before adding GSK-3β. An inhibitor was then introduced into the enzyme-doped column to assess kinase-specific retention and to determine the possibility of conducting affinity screening assays.

1.6 Thesis Outline

This thesis consists of two chapters with data, one of which is to be submitted for publication. Chapter 2 explains the optimization of the solution-based ESI-MS/MS GSK-3β assay, as well as its application towards inhibitor screening. Suitable salt/ buffer concentrations and parameters for ESI-MS work are determined first, followed by the statistical validation of the method and concluding with the description of kinase activity inhibition detection in a semi-automated inhibitor screen using synthetic compound libraries. Chapter 3 discusses the solid-phase assays performed with sol-gel immobilized GSK-3β. Enzyme leaching experiments performed with the protein entrapped in sol-gel

monoliths are demonstrated. The non-specific binding characteristics of selected GSK-3β inhibitors are discussed along with a basic test of kinase activity in a sol-gel column.

Chapter 5 lists the conclusions and offers an outlook of future work.

1.7 References

1. Doble, B.W., and Woodgett, J.R. (2003) GSK-3: tricks of the trade for a multi-tasking kinase, *J. Cell Sci. 116*, 1175–1186.

2. Cohen, P., and Goedert, M. (2004) GSK-3 inhibitors: development and therapeutic potential, *Nat.Rev. Drug Discov. 3*, 479–487.

3. Dajani, R., Fraser, E., Roe, S.M., Young, N., Good, V., Dale, T.C., and Pearl, L.H. (2001) Crystal structure of glycogen synthase kinase 3β: structural basis for phosphate-primed substrate specificity and autoinhibition, *Cell 105*, 721–732.

4. Cohen, P., and Frame, S. (2001) The renaissance of GSK-3, *Nat. Rev. Mol. Cell Biol. 2*, 769–776.

5. Kockeritz, L., Doble, B., Patel, S., and Woodgett, J.R. (2006) Glycogen synthase kinase-3 – an overview of an over-achieving protein kinase, *Curr. Drug Targ. 7*, 1377–1388.

6. Stambolic, V., Ruel, L., and Woodgett, J.R. (1996) Lithium inhibits glycogen synthase kinase-3 activity and mimics Wingless signaling in intact cells, *Curr. Biol. 6*, 1664–1668.

7. Ryves, W.J., Dajani, R., Pearl, L., and Harwood, A.J. (2002) Glycogen synthase kinase-3 inhibition by lithium and beryllium suggests the presence of two magnesium binding sites, *Biochem. Biophys. Res. Commun. 290*, 967–972.

8. McManus, E.J., Sakamoto, K., Armit, L.J., Ronaldson, L., Shpiro, N., Marquez, R., and Alessi, D.R. (2005) Role that phosphorylation of GSK-3 plays in insulin and Wnt signaling defined by knockin analysis, *EMBO J. 24*, 1571–1583.

9. Versteeg, H.H., Nijhuis, E., van den Brink, G.R., Evertzen, M., Pynaert, G.M., van Deventer, S.J., Coffer, P.J., and Peppelenbosch, M.P. (2000) A new phosphospecific cell-based ELISA for p42/p44 mitogen-activated protein kinase (MAPK), p38 MAPK, protein kinase B and cAMP-response-element-binding protein, *Biochem. J. 350*, 717–722.

10. Koresawa, M., and Okabe, T. (2004) High-throughput screening with quantitation of ATP consumption: a universal non-radioisotope, homogeneous assay for protein kinase, *Assay Drug Develop. Technol. 2*, 153–160.

11. Boehr, D.D., Farley, A.R., LaRonde, F.J., Murdock, T.R., Wright, G.D., and Cox, J.R. (2005) Establishing the principles of recognition in the adenine-binding region of an aminoglycoside antibiotic kinase [APH(3')-IIIa], *Biochemistry 44*, 12445–12453.

12. Zhang, W.X., Ruixiu, W., Wisniewski, D., Marcy, A.I., LoGrasso, P., Lisnock, J.-M., Cummings, R.T., and Thompson, J.E. (2005) Time-resolved Forster resonance energy transfer assays for the binding of nucleotide and protein substrates to p38α protein kinase, *Anal. Biochem. 343*, 76–83.

13. Sadler, T.M., Achilleos, M., Ragunathan, S., Pitkin, A., LaRocque, J., Morin, J., Annable, R., Greenberger, L.M., Frost, P., and Zhang, Y. (2004) Development and comparison of two nonradioactive kinase assays for I kappa B kinase, *Anal. Biochem. 326*, 106–113.

14. Kim, A.J., Shi, Y., Austin, R.C., and Werstuck, G.H. (2005) Valproate protects cells from ER stress-induced lipid accumulation and apoptosis by inhibiting glycogen synthase kinase-3, *J. Cell Sci. 118*, 89–99.

15. Steinberg, T.H., Agnew, B.J., Gee, K.R., Leung, W.Y., Goodman, T., Schulenberg, B., Hendrickson, J., Beechem, J.M., Haugland, R.P., and Patton, W.F. (2003) Global quantitative phosphoprotein analysis using Multiplexed Proteomics technology, *Proteomics 3*, 1128–1144.

16. Rupcich, N., Green, J.R., and Brennan, J.D. (2005) Nanovolume kinase inhibition assay using a sol-gel-derived multicomponent microarray, *Anal. Chem. 77*, 8013–8019.

17. Martin, K., Steinberg, T.H., Cooley, L.A., Gee, K.R., Beechem, J.M., and Patton, W.F. (2003) Quantitative analysis of protein phosphorylation status and protein kinase activity on microarrays using a novel fluorescent phosphorylation sensor dye, *Proteomics 3*, 1244–1255.

18. Rininsland, F., Xia, W., Wittenburg, S., Shi, X., Stankewicz, C., Achyuthan, K., McBranch, D., and Whitten, D. (2004) Metal ion-mediated polymer superquenching for highly sensitive detection of kinase and phosphatase activities, *Proc. Natl. Acad. Sci. USA 101*, 15295–15300.

19. McCauley, T.J., Stanaitis, M.L., Savage, M.D., Onken, J., and Millis, S.Z. (2003) IQ™ technology: development of a universal, homogeneous method for high-throughput screening of kinase and phosphatase activity, *J. Assoc. Lab. Autom. 8*, 36–

40.

20. Klumpp, M., Boettcher, A., Becker, D., Meder, G., Blank, J., Leder, L., Forstner, M., Ottl, J., and Mayr, L.M. (2006) Readout technologies for highly miniaturized kinase assays applicable to high-throughput screening in 1536-well format, *J. Biomol. Screen 11*, 617–633.

21. Turek, T.C., Small, E.C., Bryant, R.W., Adam, W., and Hill, G. (2001) Development and validation of a competitive AKT serine/threonine kinase fluorescence polarization assay using a product-specific anti-phospho-serine antibody, *Anal. Biochem. 299*, 45–53.

22. Annis, D.A., Nazef, N., Chuang, C.C., Scott, M.P., and Nash, H.M. (2004) A general technique to rank protein-ligand binding affinities and determine allosteric versus direct binding site competition in compound mixtures, *J. Am. Chem. Soc. 126*, 15495–15503.

23. Moy, F.J., Haraki, K., Mobilio, D., Walker, G., Powers, R., Tabei, K., Tong, H., and Siegel, M.M. (2001) MS/NMR: a structure-based approach for discovering protein ligands and for drug design by coupling size exclusion chromatography, mass spectrometry, and nuclear magnetic resonance spectroscopy, *Anal. Chem. 73*, 571–581.

24. Davidson, W., Hopkins, J.L., Jeanfavre, D.D., Barney, K.L., Kelly, T.A., and Grygon, C.A. (2003) Characterization of the allosteric inhibition of a protein-protein interaction by mass spectrometry, *J. Am. Soc. Mass Spectrom. 14*, 8–13.

25. Zhao, Y.-Z., van Breemen, R.B., Nikolic, D., Huang, C.-R., Woodbury, C.P., Schilling, A., and Venton, D.L. (1997) Screening solution-phase combinatorial libraries using pulsed ultrafiltration/electrospray mass spectrometry, *J. Med. Chem. 40*, 4006–4012.

26. Dunayevskiy, Y.M., Lyubarskaya, Y.V., Chu, Y.-H., Vouros, P., and Karger, B.L. (1998) Simultaneous measurement of nineteen binding constants of peptides to vancomycin using affinity capillary electrophoresis-mass spectrometry, *J. Med. Chem. 41*, 1201–1204.

27. Chan, N.W.C., Lewis, D.F., Rosner, P.J., Kelly, M.A., and Schriemer, D.C. (2003) Frontal affinity chromatography-mass spectrometry assay technology for multiple stages of drug discovery: applications of a chromatographic bionsensor, *Anal. Biochem. 319*, 1–12.

28. Slon-Usakiewicz, J.J., Ng, W., Dai, J.R., Pasternak, A., and Redden, P.R. (2005) Frontal affinity chromatography with MS-detection (FAC-MS) in drug discovery,

Drug Discov. Today 10, 409–416.

29. Geoghegan, K.F., and Kelly, M.A. (2005) Biochemical applications of mass spectrometry in pharmaceutical drug discovery, *Mass Spec. Rev. 24*, 347–366.

30. Bertucci, C., Bartolini, M., Gotti, R., and Andrisano, V. (2003) Drug affinity to immobilized target bio-polymers by high-performance liquid chromatography and capillary electrophoresis, *J. Chromatogr. B 797*, 111–129.

31. Ozbal, C.C., LaMarr, W.A., Linton, J.R., Green, D.F., Katz, A., Morrison, T.B., and Brenan, C.J. (2004) High throughput screening via mass spectrometry: a case study using acetylcholinesterase, *Assay Drug Develop. Technol. 2*, 373–381.

32. de Boer, A.R., Letzel, T., van Elswijk, D.A., Lingeman, H., Niessen, W.M., and Irth, H. (2004) On-line coupling of high-performance liquid chromatography to a continuous-flow enzyme assay based on electrospray ionization mass spectrometry, *Anal. Chem. 76*, 3155–3161.

33. Cardoso, C.L., Lima, V.V., Zottis, A., Oliva, G., Andricopulo, A.D., Wainer, I.W., Moaddel, R., and Cass, Q.B. (2006) Development and characterization of an immobilized enzyme reactor (IMER) based on human glyceraldehyde-3-phosphate dehydrogenase for on-line enzymatic studies, *J. Chromatogr. A 1120*, 151–157.

34. Bartolini, M., Andrisano, V., and Wainer, I.W. (2003) Development and characterization of an immobilized enzyme reactor based on glyceraldehyde-3-phosphate dehydrogenase for on-line enzymatic studies, *J. Chromatogr. A 987*, 331–340.

35. Bartolini, M., Cavrini, V., and Andrisano, V. (2005) Choosing the right chromatographic support in making a new acetylcholinesterase-micro-immobilized enzyme reactor for drug discovery, *J. Chromatogr. A 1065*, 135-144.

36. Hodgson, R.J., Besanger, T.R., Brook, M.A., and Brennan, J.D. (2005) Inhibitor screening using enzyme-reactor chromatography/mass spectrometry, *Anal. Chem. 77*, 7512–7519.

37. Besanger, T.R., Hodgson, R.J., Green, J.R., and Brennan, J.D. (2006) Immobilized enzyme reactor chromatography: optimization of protein retention and enzyme activity in monolithic silica stationary phases, *Anal. Chim. Acta 564*, 106–115.

38. Hodgson, R.J., Brook, M.A., and Brennan, J.D. (2005) Capillary-scale monolithic immunoaffinity columns for immunoextraction with in-line laser-induced fluorescence detection, *Anal. Chem. 77*, 4404–4412.

39. Yamashita, M., and Fenn, J.B. (1984) Electrospray ion source. Another variation on the free-jet theme, *J. Phys. Chem. 88*, 4451–4459.

40. Agarwal, R.P. (1982) Inhibitors of adenosine deaminase, *Pharmacol. Therap. 17*, 399–429.

41. Besanger, T.R., Easwaramoorthy, B., and Brennan, J.D. (2004) Entrapment of highly active membrane-bound receptors in macroporous sol-gel derived silica, *Anal. Chem. 76*, 6470–6475.

42. Laiko, V.V., Baldwin, M.A., and Burlingame, A.L. (2000) Atmospheric pressure matrix-assisted laser desorption/ionization mass spectrometry, *Anal. Chem. 72*, 652–657.

43. Ohkubo, M. (2007) Superconductivity for mass spectroscopy, *IEICE Trans. Electron. E90-C*, 550-555.

44. Min, D.-H., Su, J., and Mrksich, M. (2004) Profiling kinase activities by using a peptide chip and mass spectrometry, *Angew. Chem. Int. Ed. 43*, 5973–5977.

45. Min, D.-H., Tang, W.-J., and Mrksich, M. (2004) Chemical screening by mass spectrometry to identify inhibitors of anthrax lethal factor, *Nat. Biotechnol. 22*, 717–723.

46. Min, D.-H., Yeo, W.-S., and Mrksich, M. (2004) A method for connecting solution-phase enzyme activity assays with immobilized format analysis by mass spectrometry, *Anal. Chem. 76*, 3923–3929.

47. Braun, S., Rappoport, S., Zusman, R., Avnir, D., and Ottolenghi, M.(1990) Biochemically active sol-gel glasses: the trapping of enzymes, *Mater. Lett. 61*, 2843–2846.

48. Zusman, R., and Zusman, I. (2001) Glass fibers covered with sol-gel glass as a new support for affinity chromatography columns: a review, *J. Biochem. Biophys. Methods 49*, 175–187.

49. Kato, M., Onda, Y., Sakai-Kato, K., and Toyo'oka, T. (2006) Simultaneous analysis of cationic, anionic, and neutral compounds using monolithic CEC columns, *Anal. Bioanal. Chem. 386*, 572–577.

50. Sakai-Kato, K., Kato, M., and Toyo'oka, T. (2003) Creation of an on-chip enzyme reactor by encapsulating trypsin in sol-gel on a plastic microchip, *Anal. Chem. 75*, 388–393.

51. Sakai-Kato, K., Kato, M., Nakakuki, H., and Toyo'oka, T. (2003) Investigation of structure and enantioselectivity of BSA-encapsulated sol-gel columns prepared for capillary electrochromatography, *J. Pharm. Biomed. Anal. 31*, 299–309.

52. Brook, M.A., Chen, Y., Guo, K., Zhang, Z., and Brennan, J.D. (2004) Sugar-modified silanes: precursors for silica monoliths, *J. Mater. Chem. 14*, 1469–1479.

53. Kato, M., Sakai-Kato, K., and Toyo'oka, T. (2005) Silica sol-gel monolithic materials and their use in a variety of applications, *J. Sep. Sci. 28*, 1893–1908.

Chapter 2

Evaluation of the ESI-MS/MS Method for Screening of GSK-3β Inhibitors

This chapter was based on work that was solely performed by me with input and direction from Dr. Brennan. Dr. Werstuck assisted me in the proper training required for performing radioisotope-based assays. I wrote the first draft of the manuscript and Dr. Brennan provided editorial input to generate the final draft of the paper. This chapter is targeted for submission to *Biochemistry*.

Abstract

Glycogen synthase kinase-3β (GSK-3β) is involved in the hyperphosphorylation of previously phosphorylated (primed) substrates, and is currently assayed using an approach based on the incorporation of γ-^{32}P radiolabelled isotopes into substrate peptides. The requirement to detect hyperphosphorylation of a primed substrate poses a particular challenge for development of a high throughput screening assay, as many current kinase assays are designed to produce a signal in the presence of any phosphorylation site, and thus are only suitable for unphosphorylated substrates. Herein, we have developed an electrospray ionization – tandem mass spectrometry (ESI-MS/MS) assay to allow for direct detection of a hyperphosphorylated product which is formed in a solution reaction involving a primed peptide substrate (GSM peptide) and GSK-3β. Optimum reaction conditions (level of Mg^{2+}, buffer type, ionic strength, pH, enzyme concentration and reaction time) were established to both maintain the activity of GSK-3β and allow for substrate and product quantification using the ESI\-MS/MS. We show that the MS-based assay allows for rapid determination of GSK-3β activity from reaction volumes of ~40 μL, can be used to assess IC_{50} values and the site of action of known inhibitors, and can be used for automated screening of small molecules mixtures to identify inhibitors of GSK-3β.

2.1 Introduction

Phosphorylation is a key protein post-translational modification that controls a variety of regulatory processes in mammalian cells.[1] Indeed, kinases have been implicated in a wide range of disease states, and as such are highly touted as potential targets for drug

development.[2,3] A particularly important member of this family is the serine/threonine kinase, Glycogen Synthase Kinase 3 (GSK-3), which plays an intricate role within the framework of mammalian cellular metabolism, and is involved in many metabolic regulatory pathways. In addition to its role in the regulation of glycogen metabolism,[4] it is now known that GSK-3 is involved in cytoskeletal regulation,[5] cell cycle progression,[6,7] apoptosis,[8] cell fate and speciation,[9] and transcriptional/ translational initiation.[10,11] Altered GSK-3 activity, normally involving hyperphosphorylation of its targets, can contribute to a number of pathological processes including bipolar mood disorder,[12-14] schizophrenia,[15] heart disease,[16,17] neurodegeneration[18] Alzheimer's disease[19,20] and diabetes mellitus[19,21] Its involvement in Alzheimer's disease is thought to stem from its role (in conjunction with CDK6 and MARK) in the hyperphosphorylation of tau. The role of GSK-3β as the key isoform responsible for hyperphosphorylation of tau has been unequivocally established by Takashima *et. al. via* GSK-3β anti-sense treatment and PtdIns(3,4,5)P_3 inhibition studies.[22] As a consequence, there is a clear need for the development of potent and selective inhibitors of GSK-3β.

A complication in screening for inhibitors of GSK-3 is that the enzyme has an unusual preference for target proteins that have undergone a previous phospho-priming event; the enzyme generally recognizes substrates with a Ser-Xaa-Xaa-Xaa-Ser(P) motif.[23,24] A further complication is the need to target the primed substrate binding site rather than the ATP binding site so as to avoid dysregulation of other pathways regulated by GSK-3β, such as the Wnt signaling pathway.[24] This indicates that a suitable assay must be able to follow the formation of hyperphosphorylated products and assess the site of action of potential inhibitors.

At present, there are a wide range of different kinase assays that are available based on following loss of reactants (ATP), production of products (ADP or phosphorylated substrates), or displacement assays involving competition between test compounds and a suitably labelled ligand that can bind to the active site of the kinase.[25] These include: 1) cell based assays;[26] 2) ATP dependent assays (colorimetric, fluorescent and bioluminescent readouts);[25] 3) LANCE™ antibody based systems (time-resolved fluorescence resonance energy transfer (FRET) readout);[27] 4) radioassay methods; 5) ligand displacement assays (fluorescence polarization or FRET[28,29]) and; 6) phospho-specific staining methods (AlphaScreen™,[30] iron quenching,[31] IMAP,[32] Pro-Q™ Diamond stain[33]).

However, most of these assays are either unable to discriminate primed substrates from hyperphosphorylated product (i.e., LANCE™ or phosphostaining methods), require secondary assays to reduce false positives (i.e., coupled enzyme assays for ATP), or require significant manipulation of the intracellular machinery (i.e., knock-out or knock-in experiments) to be able to provide specific information regarding the inhibition of GSK-3β. Radioassay methods can be used to assess hyperphosphorylation of primed substrates by GSK-3β,[34] but such assays are not scaleable to high-throughput screening of large compound collections and have significant issues related to the use and disposal of radioactive materials. Hence, there is a need for new screening technologies to allow rapid discovery of new inhibitors of GSK-3β.

In recent years, there have been several reports on the use of mass spectrometry-based assays for both evaluation of enzyme activity and screening of enzyme inhibitors.[35] Several groups have described studies where enzyme reactions were carried out in wells

or other vessels containing the free enzyme, followed by off-line MS analysis of substrates, products and/or inhibitors to evaluate enzyme activity and ligand binding.[36-40] Other approaches have used immobilized ligands to screen enzymatic activity, with MALDI/MS providing the ability to detect conversion of the ligands.[41] Still other methods have utilized flow-through reactors wherein both the enzyme and substrate/inhibitor flow through a reaction loop followed by infusion of all components into an ESI/MS system to monitor enzyme activity,[42] or immobilized enzyme reactors interfaced off-line to MALDI/MS[43] or on-line to ESI-MS/MS[44] for evaluation of enzyme activity and inhibition. Several affinity screening formats have also been coupled with MS detection,[45] using methods such as gel permeation chromatography[46], size-exclusion chromatography,[47] pulsed ultrafiltration,[48] affinity capillary electrophoresis[49] or frontal affinity chromatography[50] (FAC-MS). However, such methods do not provide functional information on enzyme activity and require appropriate competitive ligands to assess site of action.

Two recent papers have highlighted the potential of MS for following the reactions of kinases. Irth and co-workers reported on an ESI-MS assay for protein kinase A, and showed that appropriate conditions could be obtained to allow infusion of the kinase reaction components into the MS for quantitative determination of enzyme activity and inhibition.[51] O'Gorman and co-workers reported on the use of SELDI (Surface Enhanced Laser Desorption Ionization) MS for assessment of GSK-3 activity from cell lysates, and showed the potential of the MS method to discriminate primed substrates and hyperphosphorylated products.[52] However, neither of these studies explored the use of

MS for assessing the site of action of inhibitors or for semi-automated screening of compound mixtures.

This study focuses on the development of an ESI-MS/MS method for screening GSK-3β activity and inhibition. This kinase assay utilizes a peptide substrate derived from glycogen synthase (GSM peptide) that has a serine residue at a position equivalent to the GSK-3 phosphorylation site on GS (position *n*), and phosphoserine at the *n*+4 position. The assay involves performing the kinase reaction in an optimized MS compatible buffer which is simply quenched with an acidic methanol solution and immediately subjected to ESI/MS/MS analysis with no further sample treatment. The assay allows for rapid, quantitative assessment of GSK-3β activity, determination of inhibition constants (IC_{50} or K_I), and can be used to determine the site of action of inhibitors. We also show that interfacing to an autosampler provides a platform for semi-automated screening of small molecule mixtures to identify inhibitors of GSK-3β.

2.2 Experimental Section

2.2.1 Materials

Histidine-tagged recombinant rabbit glycogen synthase kinase 3β (GSK-3β) (15 units/μg protein where 1 unit will transfer one pmol of phosphate from ATP to phosphatase inhibitor 2 per min at pH 7.5 at 30°C), SB-415286 and 10 kDa poly(ethylene glycol) (PEG) were purchased from Sigma-Aldrich (Oakville, Ontario, Canada). GSK-3β Inhibitor I and GSK-3β Inhibitor II were purchased at Calbiochem (San Diego, California, USA). HPLC grade water was purchased from Caledon Laboratory Chemicals (Georgetown, Ontario, Canada). Synthetic muscle glycogen synthase 1 peptide (GSM)

(structure: Arg-Arg-Arg-Pro-Ala-Ser-Val-Pro-Pro-Ser-Pro-Ser-Leu-Ser-Arg-His-Ser-pSer-His-Gln-Arg-Arg (2673 Da, pSer = phosphoserine)) was purchased from Upstate USA (Charlottesville, VA, USA). γ-^{32}P ATP and ACS aqueous scintillation cocktail were obtained from GE Healthcare Bio-Sciences (Baie d'Urfe, Quebec, Canada). C96 microwell plates were purchased from VWR International (Mississauga, Ontario, Canada). All reagents were used as received. Other compounds listed in Supplementary Table 2.3 were from commercial and synthetic sources.

2.2.2 GSK-3β Reaction Optimization

Kinase activity was measured by including 62.5 μM GSM substrate and 0.5 μCi/μl [γ-^{32}P] ATP with 52.5 nM of recombinant GSK-3β in a reaction mixture containing NH_4OAc (1-21 mM), MgOAc (0-2.5 mM) and 125 μM ATP in a total volume of 40 μl. After 60 minutes, the samples were spotted onto Whatman P81 phosphocellulose paper and washed three times with 0.75% o-phosphoric acid and once with acetone. ^{32}P incorporation onto the substrate was then determined by scintillation counting.

2.2.3 LC/MS Settings

Mobile phase delivery for substrate/product signal optimization studies was performed with a 1.0 mL, 4.6 mm i.d. Hamilton syringe using an AB/Sciex Q-Trap Mass Spectrometer controlled by Analyst v.1.4 software. Parent/daughter ion signals were followed using Q1 & MS2 modes of analysis in positive ion mode under the following conditions: Curtain Gas = 45.0, Collision gas = low, Ion Spray Voltage = 5000 V, Temperature = 175 °C, Ion Source Gas 1 = 40.0, Ion Source Gas 2 = 40.0. Specific

MS/MS parameters for each ion pair are provided in the supplementary data section (Table 2.1). The total scan time was 5 seconds per point.

Species	Q1 (m/z)	Q3 (m/z)	DP (V)	EP (V)	CE (V)	CXP (V)
GSM	535	515	30	7	15	6
pGSM	551	535	30	7	15	6

Table 2.1: Specific MS/MS parameters for each ion pair analyzed via ESI-MS. The total scan time was 5 seconds per point.

2.2.4 ESI-MS Signal Optimization

62.5 μM GSM was added to 0, 0.8, 1.6, 4 and 8 mM MgOAc in 6 mM NH_4OAc, pH 7.4 in a total volume of 40 μl. The GSM Q1 MS signal was detected through direct injection at 5 μL/min after diluting the samples to 120 uL with MeOH. The ratio of the GSM signal over the average of the noise was then calculated for all samples and normalized to the control value obtained using 0 mM MgOAc.

2.2.5 GSK-3β Solution-Based ESI-MS Reproducibility Assays

Kinase activity was measured by including 52.5 nM of recombinant GSK-3β in a reaction mixture containing 62.5 μM GSM substrate, 6 mM NH_4OAc/0.8 or 1.6 mM MgOAc, pH 7.4 and 125 μM ATP in a total volume of 40 μl. After a set incubation time of 1 hour, the samples were diluted to 120 μL (syringe) or 240 μL (autosampler) with MeOH and injected directly or delivered via a LC pump/autosampler into the ESI-MS at 5 μL/min, where the substrate and product signals were monitored in MS2 and multiple

reaction monitoring (MRM) modes, respectively. 10 samples for low control (-GSK-3β) and high control (+GSK-3β) were included in both the manual and semi-automated Z' assays. The Z' factor was calculated for each assay using the formula:

$$Z' = 1 - \frac{(3\sigma_C + 3\sigma_S)}{|\mu_S - \mu_C|} \qquad (1)$$

where σ_c is the standard deviation of the low control, σ_s is the standard deviation of the high control, μ_s is the average signal of the high control and μ_c is the average signal of the low control.

2.2.6 GSK-3β IC_{50} Assays

Kinase activity was measured using the reaction mixture above with 1.6 mM MgOAc and either variable ATP concentrations (25 or 125 μM ATP with 62.5 μM GSM) or variable GSM concentrations (62.5 or 125 μM GSM with 125 μM ATP) and 0.001-100 μM SB-415286 or GSK-3β Inhibitor II or 0.1 – 200 μM GSK-3β Inhibitor I in a total volume of 40 μl. After a 1 h incubation time, the samples were diluted to 120 μL with MeOH and injected directly into the ESI-MS via the syringe pump at 5 μL/min, where substrate and product signals were detected in MS2 mode. The ratio of P/S signals for each concentration was then obtained by utilizing the daughter ion peak intensities for GSM and pGSM. In all cases the binding isotherms were fit to the Hill equation:[53]

$$B = B_0\left(\frac{B_{\max}[I]^n}{IC_{50} + [I]^n}\right) \qquad (2)$$

where B is P/S signal ratio at a given concentration of inhibitor [I], B_0 and B_{max} are the minimum and maximum P/S ratios, respectively, IC_{50} is the inflection point of the

isotherm and *n* is the Hill number which influences the pitch of the inflection and can be used to determine the number of binding sites per enzyme (assumed to be 1).

2.2.7 Mixture Screen

Reaction solutions contained 6 mM NH_4OAc/1.6 mM MgOAc, pH 7.4, 125 μM ATP, 62.5 μM GSM, 52.5 nM GSK-3β, 1 μM each of 10 compounds in a mixture (10 mixtures) (except in low control (LC) solutions which contained no enzyme, no inhibitors and in high control (HC) solutions which contained 52.5 nM GSK-3β and no inhibitors) in a total volume of 40 μL. 10 μM SB-415286 was added to Mixture 2 as a control to demonstrate GSK-3β inhibition. After a 1 h incubation time, the samples were diluted to 240 μL with pure MeOH (ACIDIC??) and placed into 1 mL sample vials sealed with septum caps. Samples were injected into the ESI-MS using a Eksigent nanoLC system interfaced to an AS-1 Autosampler. Channels A and B of the NanoLC pump (each 5 mL internal volume) were filled with 6 mM NH_4OAc/1.6 mM MgOAc, pH 7.4 buffer and used as the mobile phase for all assays with a flowrate of 5 μL/min. In a typical assay the sample in the vial was aspirated into a 250 μm id PEEK sample loop with an uptake volume of 120 μL and the mobile phase was then passed through the sample loop to introduce the sample to the MS/MS system. The GSM, pGSM and SB-415286 signals were then monitored in MRM mode. 75 μm id PEEK tubing was used elsewhere in the LC system to minimize non-specific binding of compounds, which was observed in some cases when fused silica tubing was used. Blank solutions containing only mobile phase were injected by the autosampler in between every sample vial in order to rinse the system between assays.

2.3 Results and Discussion

2.3.1 Optimization of Buffer Conditions for MS-Based Analysis of GSK-3β Activity

An important issue with MS based enzyme assays is the need to find suitable solution conditions that allow high enzyme activity and a high MS signal. However, these two requirements are often at odds with each other, since enzyme activity frequently needs a high concentration of co-factors, which tend to suppress ionization of other compounds and consequently decrease MS signal. A particular problem for GSK-3β assays is the requirement for Mg^{2+} as a co-factor.

An ideal GSK-3β buffer, suitable for ESI-MS experiments, should contain a relatively low Mg^{2+} concentration, as this salt ion readily steals charge in the ESI source mass spectrometer, leading to significantly less substrate/product ionization. The presence of high concentrations of Mg^{2+} also generates significant salt adducts by complexing with the compounds present in the ESI-MS, substantially reducing the MH^+ signal and lowering the signal to noise level in Q1 scans. An analysis of the effect of Mg^{2+} in the reaction buffer was carried out in order to determine the extent of GSM signal suppression resulting from this solution component. As seen in Fig. 2.1 (top), 0 mM MgOAc demonstrated an approximately 54:1 signal to noise ratio, while the 8 mM MgOAc only had a 5:1 S/N ratio. The presence of such high levels of MgOAc decreased the GSM signal by 90% compared to the control values (Fig. 2.1 (bottom)). Low concentrations of Mg^{2+}, such as 0.8 and 1.6 mM, should therefore be more amenable for good ESI-MS detection. However, these values must also be conducive to efficient enzyme activity, since a complete Mg^{2+} deprivation of GSK-3β would effectively inactivate the kinase.

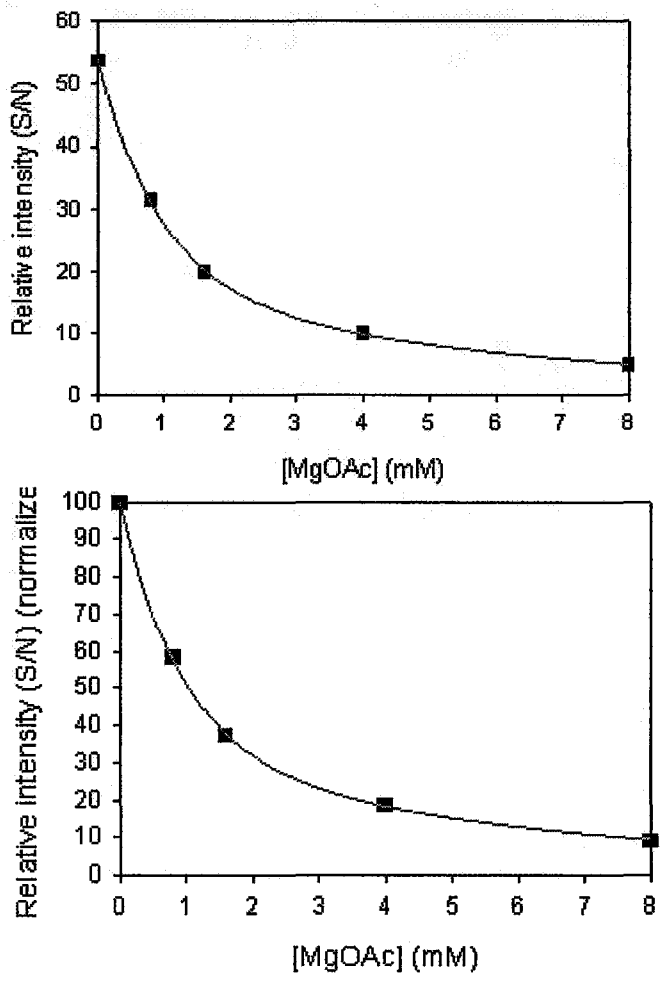

Figure 2.1: The effect of Mg^{2+} ions on GSM Q1 signal. 62.5 μM GSM in 6 mM NH_4OAc with 0, 0.8, 1.6, 4 and 8 mM MgOAc were infused into the ESI-MS at 5 μL/min via the syringe pump. GSM signal to noise ratio (top); S/N normalized to 0 mM MgOAc control (bottom).

To determine the effect of Mg^{2+} concentration on the activity of GSK-3β, a ^{32}P ATP radio assay was performed, with 62.5 μM GSM, 125 μM ATP and 52.5 nM enzyme incubated in 2 mM MOPS with 0 – 2.5 mM MgOAc. The data (Fig. 2.2 (top)) showed that the minimal concentration of Mg^{2+} needed for robust enzymatic function was 0.8 mM, as indicated by a sharp drop in GSK-3β activity below this value of MgOAc. This concentration of Mg^{2+} provided both a good S/N ratio for MS based assays and an easily detectable quantity of pGSM.

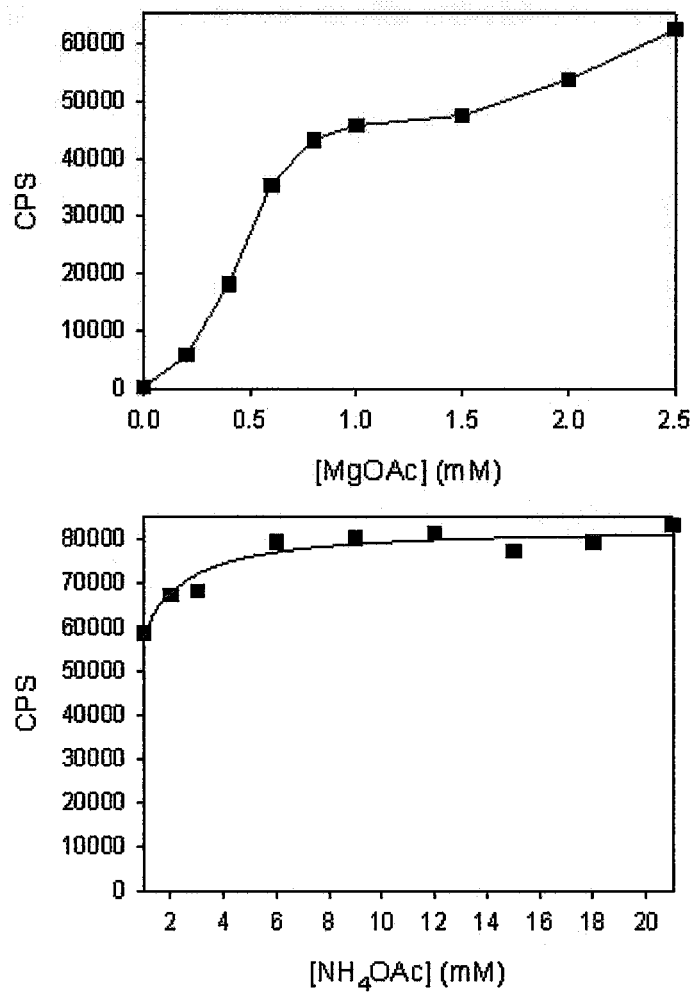

Figure 2.2: ^{32}P ATP radio assay of GSK-3β activity in solution as a function of Mg^{2+} and buffer concentrations. 0 – 2.5 mM MgOAc concentration assay (in 2 mM MOPS) (top) and 1 – 21 mM NH_4OAc concentration assay (with 0.8 mM MgOAc) (bottom).

The next step in the buffer optimization involved the assessment of the reaction buffer concentration for good enzyme activity and MS compatibility. In order to improve MS substrate and product signals in our GSK-3β assays, the previously utilized MOPS buffer was exchanged for the more volatile and MS-compatible NH_4OAc buffer. The reaction mixtures containing radio labeled ATP were then incubated with 1 – 21 mM NH_4OAc in 0.8 mM MgOAc for 1 h. [NH_4OAc] had a strong effect on enzyme activity early on, with the product signal reaching a plateau around 6 mM NH_4OAc and

remaining constant beyond this point (Fig. 2.2 (bottom)). 6 mM NH_4OAc was therefore chosen as the optimal reaction buffer concentration to use in GSK-3β assays, as any lower concentrations would result in less kinase activity, while higher concentrations could potentially contribute to ion suppression, decreasing GSM/pGSM signal intensity.

Once suitable buffer conditions were determined, GSK-3β activity in solution was assessed as a function of time using ^{32}P ATP radio assays in order to quantify enzyme activity. 62.5 μM GSM, 52.5 nM GSK-3β and 125 μM ATP were incubated with the 6 mM NH_4OAc/0.8 mM MgOAc, pH 7.4 buffer. The results of the assay, measured in product concentration, revealed a linear relationship between enzyme activity and time for the +GSK-3β reaction and essentially no signal for the negative control (–GSK-3β) reaction (Fig. 2.3). For the positive control, the quantity of pGSM reached 7 μM (~11% conversion from 62.5 μM substrate) after 2 h, indicative of a relatively slow turnover rate for GSK-3β. This is in fact favourable for monitoring enzymatic activity, as the substrate/product conversion should ideally remain at 10% or less in order to retain the initial reaction rate proportional to product concentration.

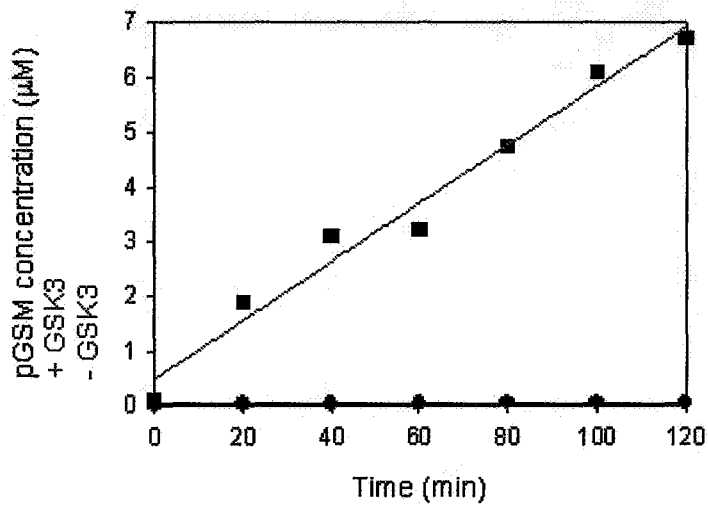

Figure 2.3: Time based ^{32}P ATP GSK-3β activity assay with 6 mM NH_4OAc/0.8 mM MgOAc, pH 7.4 and 52.5 nM GSK-3β as positive control (red) and assay with 6 mM NH_4OAc/0.8 mM MgOAc, pH 7.4 and no enzyme as negative control (blue).

2.3.2 Detection of Substrate and Product & Calibration of MS System for ESI-MS

Since GSK-3β ESI-MS based screening assays are dependent on monitoring product/substrate ratios by MS/MS, obtaining distinct and unambiguous GSM and pGSM MS precursor and product ion signals was one of the key goals in the early stages of this study. The analysis of GSM was carried out first with 62.5 μM GSM dissolved in 6 mM NH_4OAc/0.8 mM MgOAc, pH 7.4, injected into the ESI-MS at 5 μL/min. The resulting GSM Q1 spectrum (Fig. 2.4 (top)), shows a prominent peak at 535 m/z, corresponding to the expected m/z of the substrate peptide in the +5 charge state. Analysis of the parent ion in MS2 mode (Fig. 2.4 (bottom)) revealed a prominent daughter ion peak at 515 m/z, providing a useful MRM transition to monitor the presence of the GSM peptide with ESI-MS/MS.

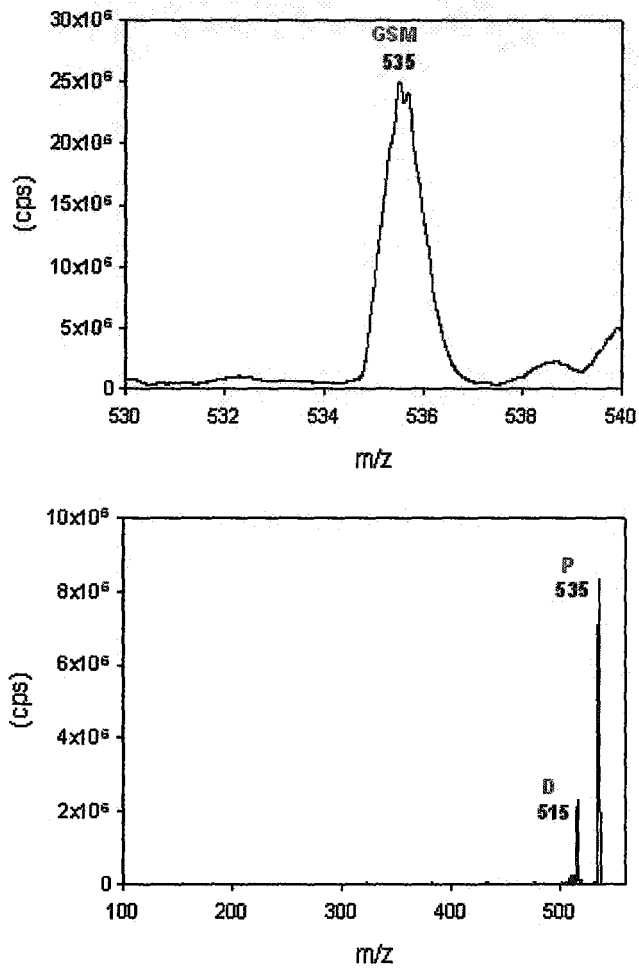

Figure 2.4: GSM Q1 (top) and MS2 (bottom) signal analysis (P = Parent/D = Daughter ion). 62.5 μM GSM in 6 mM NH_4OAc/0.8 mM MgOAc, pH 7.4 infused at 5 μL/min via the syringe pump.

To obtain a sufficient pGSM concentration for MS analysis, reaction mixtures containing 0, 52.5 nM and 525 nM GSK-3β were incubated for 80 min. MS scans of these mixtures are shown in Figure 2.5. A Q1 scan of the reaction containing 52.5 nM GSK-3β revealed the presence of a product signal with 80 mass unit shift at +5 charge state at 551 m/z (~6 x 10^6 cps) (Fig. 2.5 (middle)), indicating substrate/product conversion. As expected, a dependence on GSK-3β concentration was observed with almost no pGSM in the control solution (Fig. 2.5 (top)) and significantly more pGSM present in the reaction mixture with 10X GSK-3β concentration (Fig. 2.5 (bottom)).

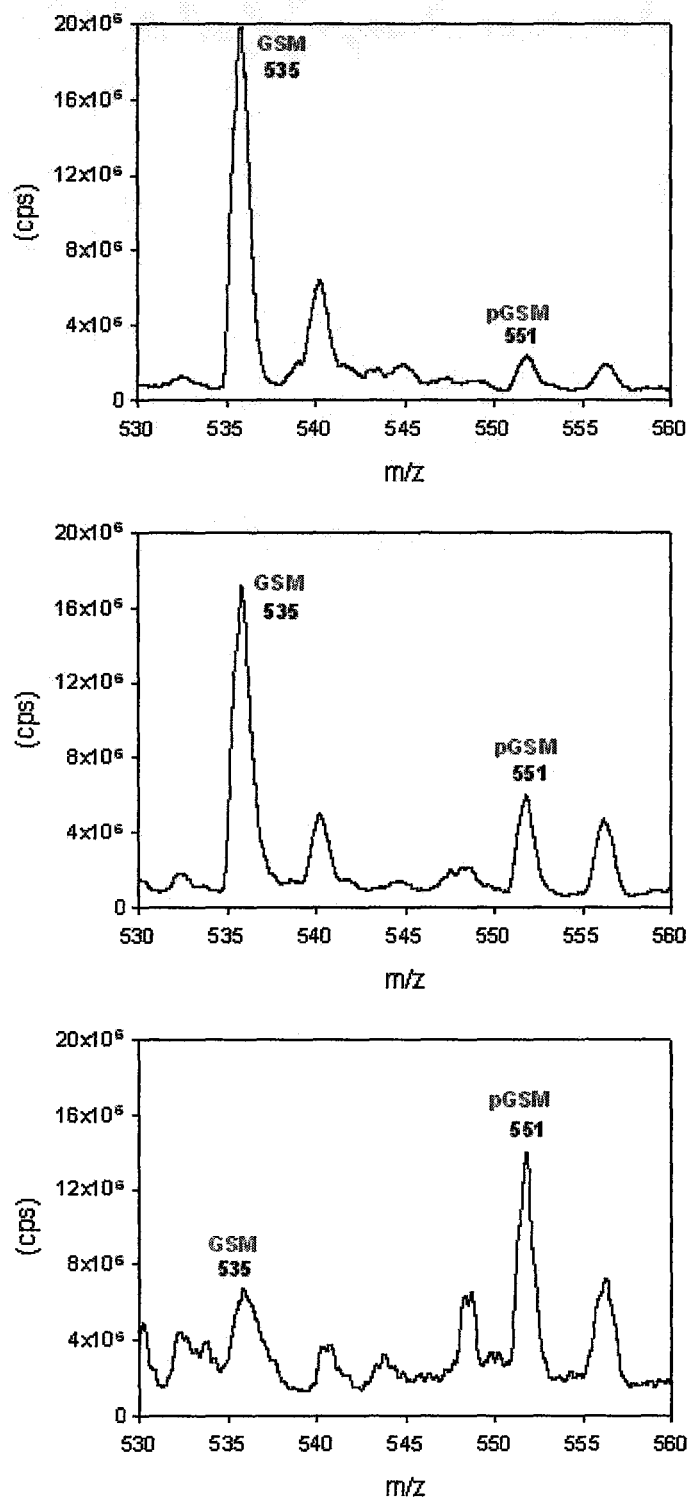

Figure 2.5: GSM & pGSM Q1 signal analysis as a function of GSK-3β concentration. Reaction enzyme concentration: 0 nM GSK-3β (top), 52.5 nM GSK-3β (middle) and 525 nM GSK-3β (bottom). 62.5 μM GSM, 125 μM ATP and 6 mM NH_4OAc/0.8 mM MgOAc, pH 7.4 buffer were used. All reactions were infused directly at 5 μL/min via the syringe pump.

Although the signal intensity of pGSM in both GSK-3β containing solutions is much higher than the control solution with no enzyme, a distinct peak at 551 m/z is still present in the control despite the absence of enzyme to generate pGSM. In each case, the parent ion at 551 m/z (Fig. 2.6 (top)) was examined in MS2 mode to acquire daughter ions. As seen in Fig. 2.6 (bottom), at 551 m/z is the pGSM parent ion, followed closely by two daughter ions at 535 m/z and 515 m/z.

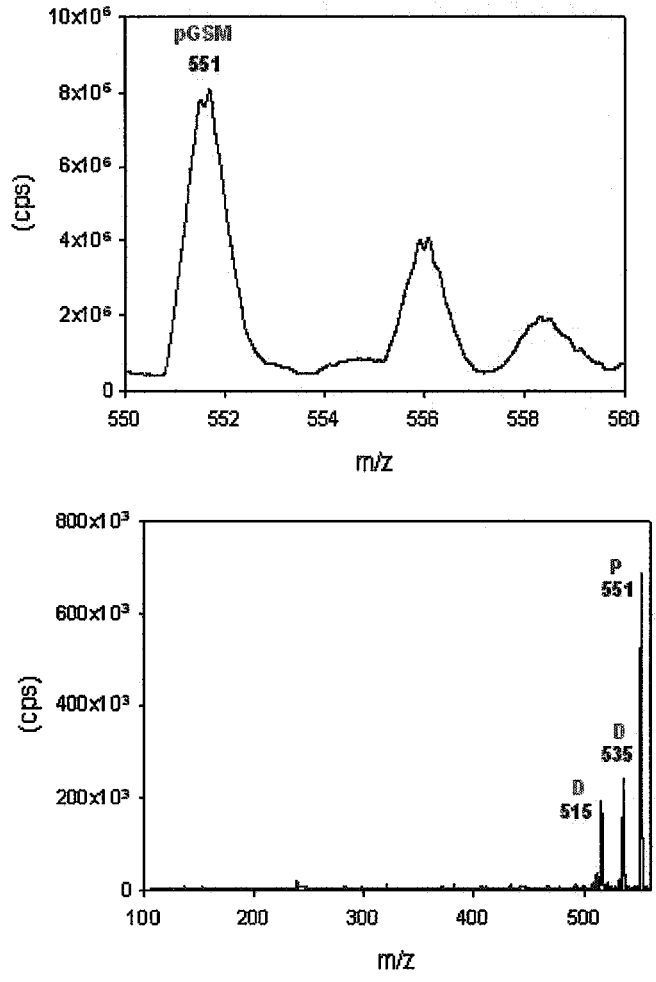

Figure 2.6: pGSM Q1 (top) and MS2 (bottom) signal analysis (P = Parent ion, D = Daughter ion). A quenched reaction solution initially containing 62.5 μM GSM, 125 μM ATP and 52.5 nM GSK-3β in 6 mM NH_4OAc/0.8 mM MgOAc, pH 7.4 was infused at 5 μL/min via the syringe pump.

The 535 m/z ion corresponds to the reversion of the peptide back to GSM, which then fragments again on its own to form the 515 m/z peak. This provides strong support for the presence of the pGSM signal at 535 m/z, as no other species would be capable of generating daughter ions that precisely overlap with the substrate signal. The presence of 535 m/z and 515 m/z daughter ions in the MS2 analysis of pGSM in the control solution thus suggests that the substrate solution contains small amounts of pGSM prior to the introduction of GSK-3β and for accurate measurement, should be subtracted as a baseline value for all pGSM data obtained in subsequent experiments. Although the origin of this pGSM is unknown, it is possible that it is a byproduct of the substrate synthesis that is not removed by purification, as the GSM substrate is only $\geq$ 90% pure (Upstate Millipore official product documentation).

2.3.3 Validation of GSK-3β Activity Using a Solution-based ESI-MS Method

The application of the solution-based ESI-MS technology for monitoring GSK-3β activity possesses many potential benefits, such as the capacity for the rapid detection of previously unknown inhibitors. To validate that the MS-based assay was accurately measuring GSK-3B activity, an enzyme concentration assay was performed. The reaction mixture containing 62.5 μM GSM, 125 μM ATP in 6 mM NH_4OAc/0.8 mM MgOAc, pH 7.4 was incubated with varying levels of GSK-3β for 10 min and then assessed for pGSM concentration. The results demonstrated a linear increase of pGSM signal with kinase concentration, as expected (Fig. 2.7).

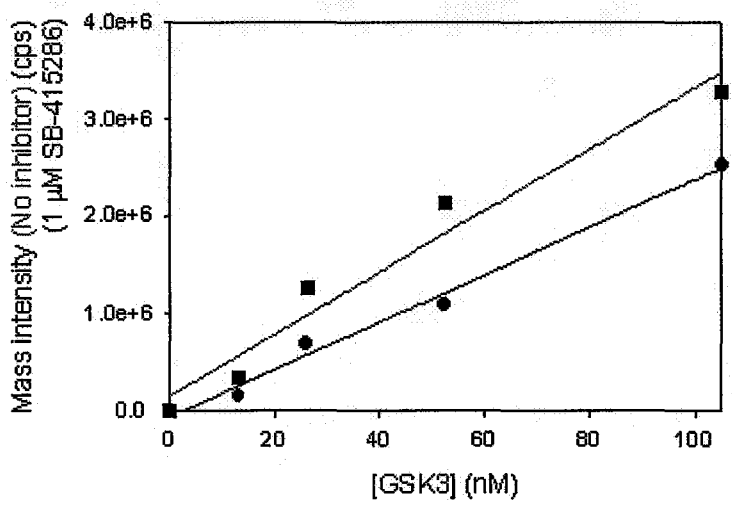

Figure 2.7: GSK-3β solution-based MS 10 min concentration-dependent activity assay. Control (red, square) and 1 µM SB-415286 (blue, circle). Data collected in MS2 mode.

In order to ensure the reliability and reproducibility of the results in GSK-3β inhibitor screening experiments, statistical validation of the solution-based MS assay was required. Application of the Z' test allowed for the determination of the statistical average and standard deviation in enzyme/no enzyme controls. Although the Z' factor can range between 0 and 1, the closer the value is to 1, the higher the level of consistency in the screen and the greater the statistical confidence in the outcome of the assay. Control reactions with and without GSK-3β were used to gather the statistical data. At this point, the concentration of Mg^{2+} in all reactions was now doubled to 1.6 mM MgOAc, as this concentration was previously demonstrated to be compatible with ESI-MS, with other experimental assays (data not shown) simultaneously recording a significant increase in kinase activity due to this change. The assays were run sequentially with both direct injection and semi-automated delivery of the methanol-quenched reaction solutions and the resulting P/S signal ratio was recorded for each reaction. The average/standard deviation for direct injection were 0.78 ± 0.06 for the GSK-3β high control and 0.14 ±

0.01 for the low control (Fig. 2.8 (top)). For semi-automated delivery, the GSK-3β high control was 0.99 ± 0.06 and low control was 0.27 ± 0.03 (Fig. 2.8 (bottom)). The corresponding Z'-factors were calculated to be 0.68 for direct injection and 0.60 for the autosampler assays – each resulting in "an excellent assay" ranking as interpreted by Zhang et al[54]. The successful statistical validation of the assay method thus allowed high confidence that the enzyme performs reproducibly over a multiple number of reactions. This approach can consequently now be applied to other GSK-3β solution based semi-automated MS experiments, such as those involving compound library mixture screening.

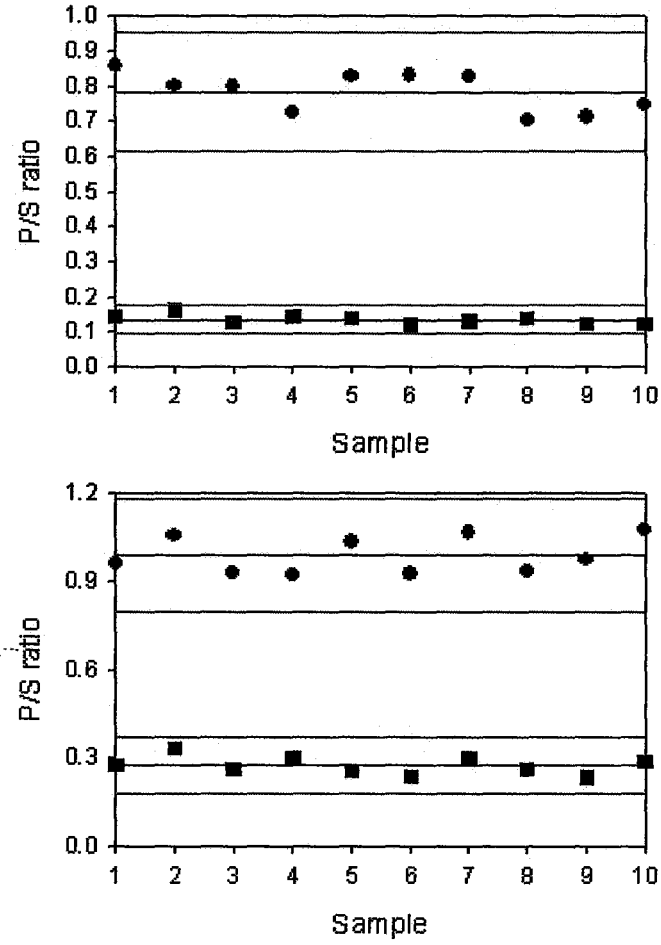

Figure 2.8: Z' analysis of the GSK-3β solution-based MS assay with direct injection (top) or autosampler (bottom). +GSK-3β control reactions (circle), -GSK-3β control reactions (square), averages (blue) and 3 standard deviations (red).

Acquisition of the IC_{50} value for the ATP-competitive inhibitor SB-415286 was performed next to demonstrate the capacity of ESI-MS to monitor the effect of inhibitor concentration on kinase activity. The experiment was conducted with 6 mM NH_4OAc/ 1.6 mM MgOAc, pH 7.4 buffer, 62.5 μM GSM, 125 μM ATP and 52.5 nM GSK-3β with 0.001-100 μM SB-415286 added to the reaction mixtures. Following a 1 h incubation period to allow a sufficient concentration of pGSM to be produced (see Fig. 2.3), the solutions were analyzed via ESI-MS and a subsequent drop in the P/S signal ratio was detected with a resulting IC_{50} of 0.81 μM (Fig. 2.9 (top)). Dropping the ATP level five-fold reduced the IC_{50} to 0.18 μM, confirming the ATP binding site to be the site of action and competitive inhibition to be the mode of action. Analysis of GSK-3β Inhibitor I, a known allosteric inhibitor, over a concentration range of 0.1 – 200 μM, demonstrated an IC_{50} value of 45 μM for the higher ATP concentration and 35 μM for the lower ATP concentration (Fig. 2.9 (middle)), as would be expected for a non-ATP competitive compound (typical errors in IC_{50} values are on the order of 10%). As a further application of this method, the evaluation of a compound with an uncharacterized mode of action, GSK-3β Inhibitor II, was performed. The inhibitor was tested with high and low ATP concentrations producing IC_{50} values of 2 μM and 1 μM, respectively. These results strongly suggest that this inhibitor is not ATP competitive, and is consistent with either allosteric or possibly mixed inhibition.

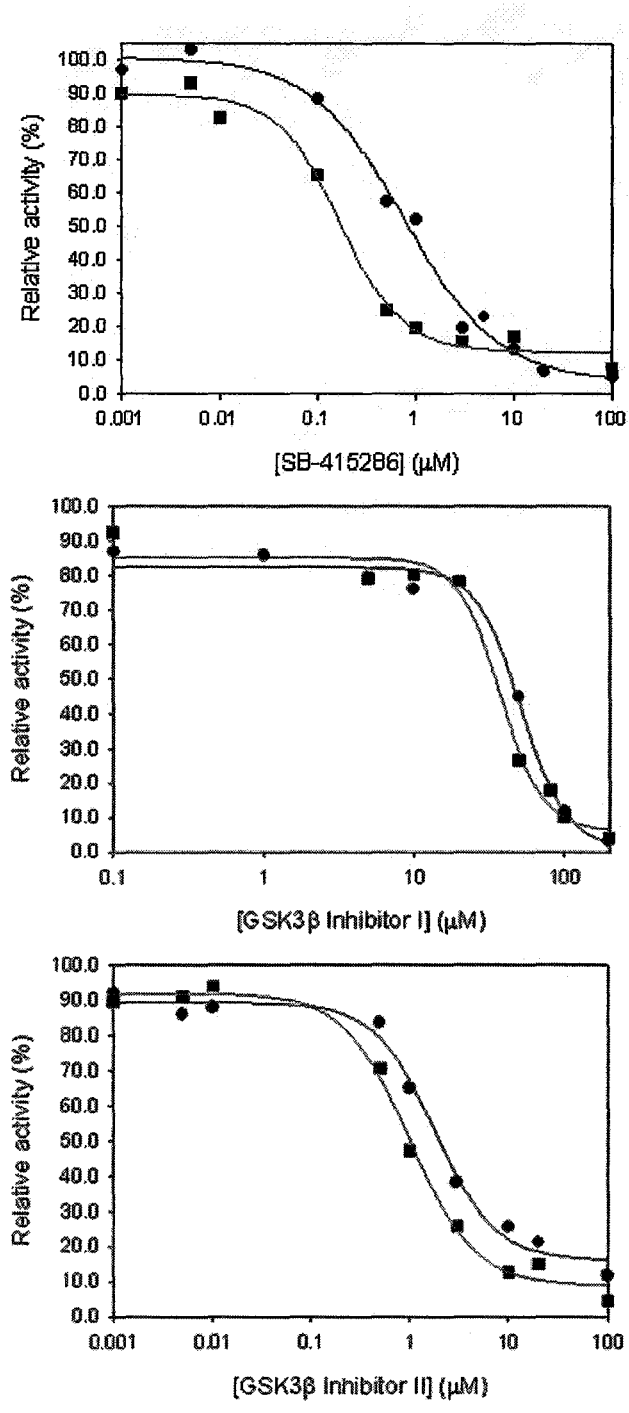

Figure 2.9: IC_{50} curves for GSK-3β kinase activity collected over a 1 x 10^{-3} to 100 μM concentration range of SB-415286 (top) and GSK-3β Inhibitor II (bottom) and over a 0.1 to 200 μM concentration range of GSK-3β Inhibitor I (middle). 62.5 μM GSM, 125 or 25 μM ATP and 52.5 nM GSK-3β were incubated in 6 mM NH_4OAc/1.6 mM MgOAc, pH 7.4 buffer for 1 h. Control (125 μM) ATP concentration – blue, (●), decreased (25 μM) ATP concentration – red, (■). Data is plotted after P/S values were applied to the Hill equation on a log scale and normalized to the control values of the uninhibited reactions.

Further evaluation of the 3 inhibitors was done using high and low levels of the GSM substrate (2-fold concentration difference). These studies yielded no substantial change in the IC_{50} values for any of the compounds tested (Table 2.2). This finding confirms not only that SB-415286 is an ATP-competitive inhibitor and that GSK-3β Inhibitor I is an allosteric inhibitor, but also suggests that the previously uncharacterized GSK-3β Inhibitor II is likely an allosteric inhibitor as well, as its mode of action was demonstrated to be largely non-competitive with respect to both ATP and GSM. These results highlight the potential of the ESI-MS/MS method to provide detailed information not only on inhibition constants but also on site of action.

Inhibitor	**Mode of action (literature)**	**IC_{50}: Low [ATP] High [ATP]**	**IC_{50}: Low [GSM] High [GSM]**	**Mode of action (experimental)**
SB-415286	ATP-competitive	0.18 μM 0.81 μM	0.81 μM 0.74 μM	ATP-competitive
GSK-3β Inhibitor I	Allosteric	35 μM 45 μM	45 μM 31 μM	Allosteric
GSK-3β Inhibitor II	Unknown	1 μM 2 μM	2 μM 3 μM	Allosteric

Table 2.2: Summary of IC_{50} experiments performed with inhibitors SB-415286, GSK-3β Inhibitor I and GSK-3β Inhibitor II. Low [ATP] – 25 μM ATP, High [ATP] – 125 μM ATP, Low [GSM] – 62.5 μM GSM and High [GSM] – 125 μM GSM.

3.4 Semi-automated ESI-MS Compound Mixture Screening

Following the establishment of IC_{50} values for GSK-3β inhibitors, the application of the solution-based ESI-MS approach towards mixture screening was the next goal. The introduction of an autosampler unit operating in tandem with the MS greatly increased

the efficiency of the assays and allowed for the automated injection of samples for screening of multiple compounds against the enzyme. However, in the absence of conventional liquid handling technology, the reactions themselves were all prepared and quenched manually, subsequently resulting in the "semi-automated" state of the assay. This step of the assay could also be readily automated using a conventional liquid handler, however this was not done for this study.

As a proof-of-concept for the autosampler-based assay, we performed a small screen of 10 mixtures containing 10 compounds each. This study was designed to demonstrate the potential of the MS-based assay for mixture screening. The 100 compounds selected for this screen were all drug-like (according to Lipinski's rules) and were either from commercial sources or were synthesized and purified to high purity (Table 2.3). Each compound was dissolved from an initial 1 μM stock in DMSO to a concentration of 1 μM in assay buffer to minimize the amount of DMSO present – this compound has previously been shown to have a deleterious effect on the electrospray process and must be minimized in ESI/MS-based assays. Final DMSO concentrations in test mixtures was typically ~0.1% (v/v). A concentration of 1 μM was chosen for screening as higher concentrations could lead to ion suppression, while lower concentrations may lead to some of the weaker inhibitors being missed in the assay.

#	Compound	#	Compound	#	Compound
1	Galanthamine	41	TB-726-1	81	JL2-57-A1
2	R-(-)-Deprenyl hydrochloride	42	TB-806-2	82	EME-231-2
3	Phenelzine sulfate salt	43	TB-814	83	EME-303-1
4	Sparteine sulfate	44	TB-846	84	EME-297-4
5	Pargyline hydrochloride	45	TB-314-2	85	JL2-63
6	Caffeine	46	TB-831-1	86	EME-231
7	Acetopromazine	47	TB-786-1	87	EME-299
8	Pyrimethamine	48	TB-748-2	88	EME-270-2
9	Sodium valproate	49	TB-784	89	EME-267
10	7326653	50	TB-853	90	JL2-16
11	Coumarin	51	FC-394	91	TB-646-1
12	Turbocuranine hydrochloride	52	FC-364	92	TB-637-5
13	Serotonin	53	FC-275	93	TB-630-1
14	(-)-Nicotine	54	FC-272	94	TB-646-3
15	Warfarin	55	FC-373	95	TB-646-4
16	Fluphenazine dihydrochloride	56	FC-268	96	TB-637-4
17	Trimethoprim	57	FC-393	97	TB-646-2
18	EHNA	58	FC-331	98	TB-642
19	Adenine	59	FC-214	99	TB-663-3
20	SB-415286	60	FC-314	100	TB-614
21	Acivicin	61	JL2-57-A4		
22	Benzamidine hydrochloride	62	JL2-57-D2		
23	Haloperidol	63	RV-1-147		
24	(-)-Sulpiride	64	JL2-57-D4		
25	Spiperone	65	JL2-57-A2		
26	Atropine	66	JL2-66B		
27	7325261	67	JL2-57-B4		
28	Tamoxifen	68	JL2-12		
29	Acetominaphen	69	RV-1-157		
30	Dextromethorphin	70	JL2-57-C5		
31	H-89	71	FC-245		
32	310618	72	FC-219		
33	Mecamylamine	73	FC-311		
34	Kynuramine dihydrobromide	74	DG-1-145B		
35	(-)-Quinpirole hydrochloride	75	SO-1-8		
36	EME-274-4	76	DG-1-14		
37	EME-285-2	77	GO-0105		
38	EME-109	78	SO-1-14		
39	EME-281-3	79	GU-252		
40	EME-297-3	80	GA-2-43		

Table 2.3: Drug-like compounds selected for the 100 compound semi-automated mixture screen. Compounds 36 to 100 are proprietary compounds taken from the Capretta small molecule collection and represent a random selection of drug-like heterocycles including maleimides, isoquinolines, benzodiazapines and pyrazines.

The results of the automated mixture screening assay are shown in Fig. 2.10. Panel A shows the raw data (P/S signal ratio) obtained during the assay, while Panel B shows a bar graph (on the same time axis) that provides the average P/S signal ratio from Panel A. Also shown on both panels is the signal obtained by monitoring the MS/MS signal from SB-415286, which was spiked into Mixture 2. Also shown are signals obtained for high controls (a sample containing no potential inhibitors) and a low control (no enzyme). The results show that both the low control and Mixture 2 resulted in a significant drop in the P/S ratio to similar levels, indicating the presence of an inhibitor, while all other samples remained at high P/S ratios. Panels C and D show the raw and processed data obtained for automated injection of each individual compound in Mixture 2, and demonstrate that it is SB-415286 (compound **20**) that is responsible for the inhibitory action observed in Mixture 2. This clearly demonstrates the ability of the MS-based assay to detect inhibitors within compound mixtures as a means for primary screening, and to subsequently deconvolute these mixtures to identify the active compound. Although the example provided involved only 100 compounds in 10 mixtures, it is possible to screen and deconvolute a considerably larger quantity of compounds per sample to increase throughput. Indeed, even in the present study it was possible to screen 100 compounds using only 20 assays (not including controls); an even better ratio of assays per compound is possible with more complex mixtures.

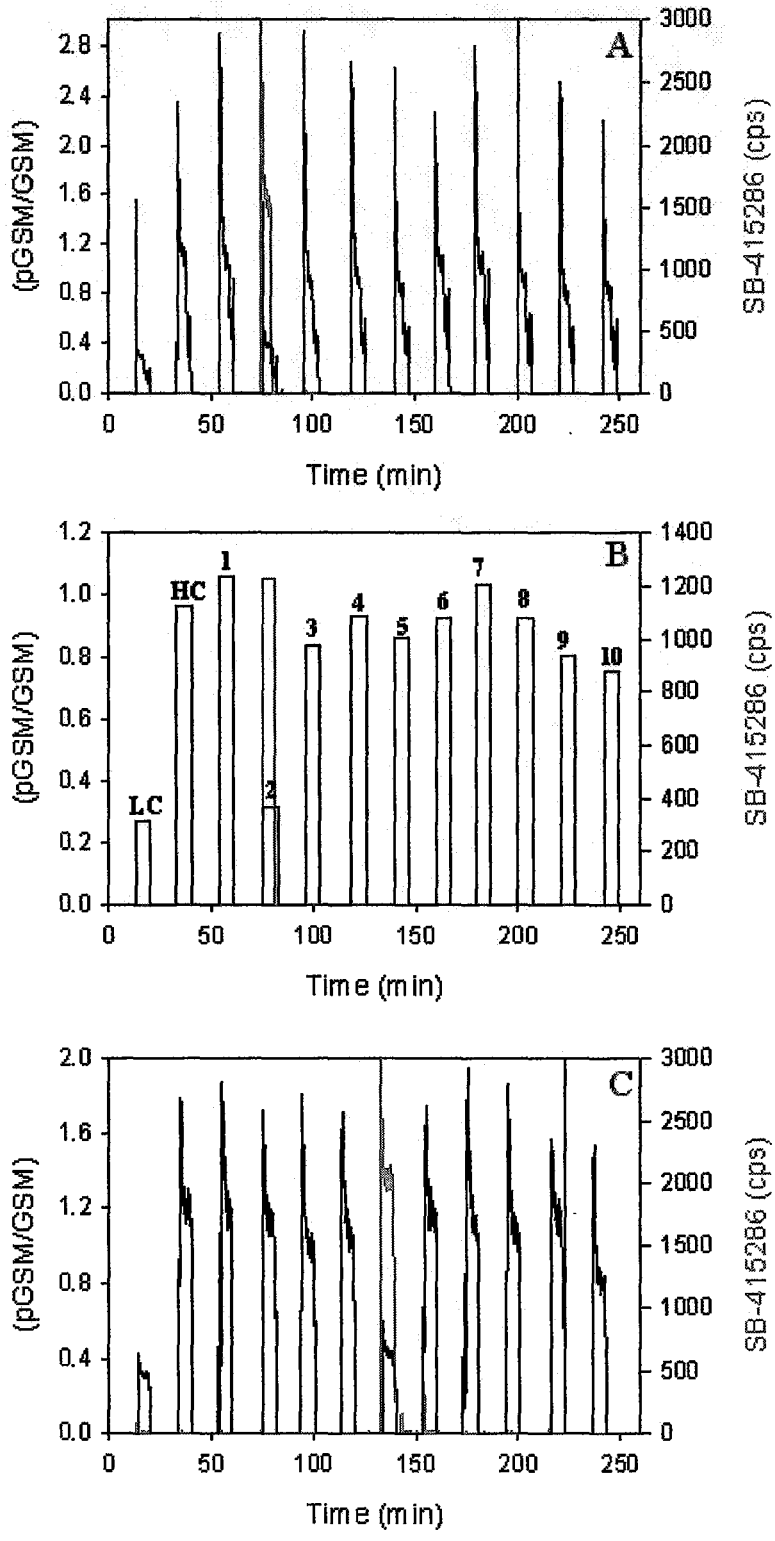
A
(pGSM/GSM)
SB-415286 (cps)
Time (min)
B
LC
HC
1
2
3
4
5
6
7
8
9
10
(pGSM/GSM)
SB-415286 (cps)
Time (min)
C
(pGSM/GSM)
SB-415286 (cps)
Time (min)

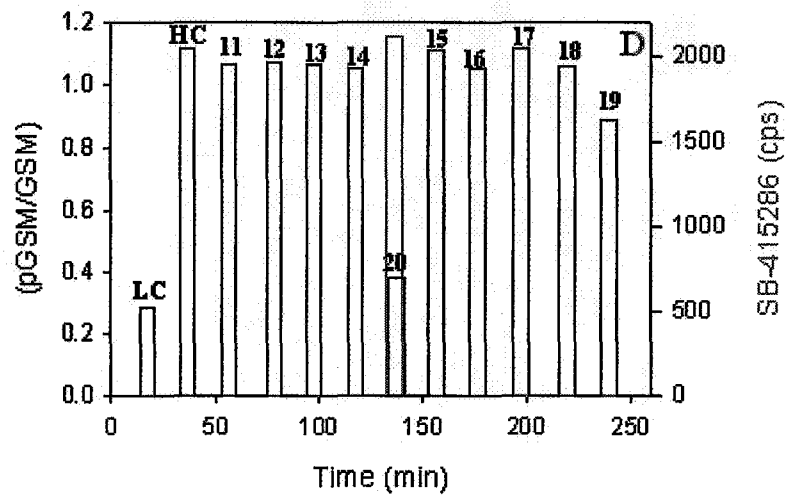

Figure 2.10: Preliminary solution-based ESI-MS analysis of a 100 compound inhibitor mixture in a screen for GSK-3β inhibitors. Black – pGSM/GSM ratio, pink – SB-415286 MRM signal trace (panels A & C). All signals averaged over their respective 6 min injection periods (panels B & D). Low control, high control, Mixture 1 – 10 (panels A & B). Low control, high control, Compound 11, 12, 13, 14, 20, 15, 16, 17, 18, 19 (panels C & D) (See Table 2.3 for compound data).

One issue with the current assay is the relatively show speed (ca 20 min per sample). The long assay time is a result of a relatively show ;flowrate (which is typical of nanoflow LC pumps) and the large injection volume. The larger volumes were used to provide sufficient time to allow for a stable MS signal. Based on the data in Figure 2.10, a shorter time of perhaps 3-4 min per point would be possible using a lower injection volume. Use of a higher flow rate pump could also provide significant improvements in assay time, but this was not possible with our existing equipment. We note that it should be possible to increase assay speed to the range of ~10 sec per sample, based on results provided by Biotrove Inc.[55] Thus, with further optimization in terms of both mixture complexity (ca. 100 compounds per mixture) and assay speed (1 mixture every 10 sec) it should be possible to screen up to 600 compounds per min, or >850,000 compounds per day per instrument (not including time for deconvolution of hits). Progress toward this goal is ongoing in our lab and the results of these studies will be presented in due course.

2.4 Conclusions

Through the optimization of GSK-3β-specific reaction parameters, such as buffer/Mg^{2+} concentrations, and GSK-3β substrate/product MS signal configuration, the development of a new, robust solution-based ESI-MS screening technology capable of monitoring changes in GSK-3β activity was possible. Unlike the majority of commonly used kinase assays, this method presents a distinct advantage in the field of chemical biology and drug screening, as it can readily distinguish between the monophosphorylated substrate and the diphosphosporylated product of GSK-3β. Its automated mode of operation also allows for more efficient drug screening as compared to the traditional ^{32}P radio-assay technique currently used to assess GSK-3β activity. IC_{50} values for specific GSK-3β inhibitors as well as a statistical validation of the assay prove the applicability of this method to other potential avenues of research such as complex mixture screening using compound libraries and natural extracts. Vast protein consumption and the lack of reusable enzyme, however, remain as practical limitations to the scaling up of the screening process. Pending further developments in sol-gel entrapment of GSK-3β, future research will emphasize kinase immobilization in solid-phase MS assays. This approach can potentially eliminate the existing obstacles mentioned above. As an alternative to the solid-state method, the application of automated liquid handling can further improve the solution-based assay. However, further optimization would be required to increase the throughput of this method prior to complete automation. The main targets of improvement include increasing mixture complexity for more effective coverage of compound libraries and reduction of injection times for the reactions as well as for the washing steps in between them. Thousands of

compounds originating from synthetic libraries and natural product extracts could then be rapidly screened, compensating for the high protein consumption. The speed and accuracy of this system should prove to be an invaluable tool in the future developments of GSK-3β research.

Acknowledgements

We thank Anna X for providing technical assistance in the performance of GSK-3β radioassays. The authors thank MDS-Sciex and the Natural Sciences and Engineering Research Council of Canada and the Canadian Institutes for Health Research for financial support of this work. JDB holds the Canada Research Chair in Bioanalytical Chemistry.

2.5 References

1. Ahn, N.G., and Resing, K.A. (2001) Toward the phosphoproteome, *Nat. Biotechnol. 19*, 317–318.

2. Hunter, T. (1995) Protein kinases and phosphatases: the yin and yang of protein phosphorylation and signaling, *Cell 80*, 225–236.

3. Ermak, G., and Davies, K.J. (2002) Calcium and oxidative stress: from cell signaling to cell death, *Mol. Immunol. 38*, 713–721.

4. Embi, N., Rylatt, D.B., and Cohen, P. (1980) Glycogen synthase kinase-3 from rabbit skeletal muscle. Separation from cyclic-AMP-dependent protein kinase and phosphorylase kinase, *Eur. J. Biochem. 107*, 519–527.

5. Hanger, D.P., Hughes, K., Woodgett, J.R., Brion, J.P., and Anderton, B.H. (1992) Glycogen synthase kinase-3 induces Alzheimer's disease-like phosphorylation of tau: generation of paired helical filament epitopes and neuronal localisation of the kinase, *Neurosci. Lett. 147*, 58–62.

6. Diehl, J.A., Cheng, M., Roussel, M.F., and Sherr, C.J. (1998) Glycogen synthase kinase-3β regulates cyclin D1 proteolysis and subcellular localization, *Genes Dev. 12*, 3499–3511.

7. Watcharasit, P., Bijur, G.N., Song, L., Zhu, J., Chen, X., and Jope, R.S. (2003) Glycogen synthase kinase-3β (GSK3β) binds to and promotes the actions of p53, *J. Biol. Chem. 278*, 48872–48879.

8. Sears, R., Nuckolls, F., Haura, E., Taya, Y., Tamai, K., and Nevins, J.R. (2000) Multiple Ras-dependent phosphorylation pathways regulate Myc protein stability, *Genes Dev. 14*, 2501–2514.

9. Kim, L., and Kimmel, A.R. (2000) GSK3, a master switch regulating cell-fate specification and tumorigenesis, *Curr. Opin. Genet. Dev. 10*, 508–514.

10. Welsh, G.I., and Proud, C.G. (1993) Glycogen synthase kinase-3 is rapidly inactivated in response to insulin and phosphorylates eukaryotic initiation factor eIF-2B, *Biochem. J. 294*, 625–629.

11. Jope, R.S., and Johnson, G.V. (2004) The glamour and gloom of glycogen synthase kinase-3, *Trends Biochem. Sci. 29*, 95–102.

12. Phiel, C.J., and Klein, P.S. (2001) Molecular targets of lithium action, *Annu. Rev. Pharmacol. Toxicol. 41*, 789–813.

13. Jope, R.S. (1999) Anti-bipolar therapy: mechanism of action of lithium, *Mol. Psychiatry 4*, 117–128.

14. Su, Y., Ryder, J., Li, B., Wu, X., Fox, N., Solenberg, P., Brune, K., Paul, S., Zhou, Y., Liu, F., and Ni, B. (2004) Lithium, a common drug for bipolar disorder treatment, regulates amyloid-beta precursor protein processing, *Biochemistry 43*, 6899–6908.

15. Kozlovsky, N., Belmaker, R.H., and Agam, G. (2002) GSK-3 and the neurodevelopmental hypothesis of schizophrenia, *Eur. Neuropsychopharmacol. 12*, 13–25.

16. Murphy, E. (2004) Inhibit GSK-3β or there's heartbreak dead ahead, *J. Clin. Invest. 113*, 1526–1528.

17. Tong, H., Imahashi, K., Steenbergen, C., and Murphy, E. (2002) Phosphorylation of glycogen synthase kinase-3β during preconditioning through a phosphatidylinositol-3-kinase--dependent pathway is cardioprotective, *Circ. Res. 90*, 377–379.

18. Kaytor, M.D., and Orr, H.T. (2002) The GSK3 β signaling cascade and neurodegenerative disease, *Curr. Opin. Neurobiol. 12*, 275–278.

19. Jope, R.S., and Johnson, G.V. (2004) The glamour and gloom of glycogen synthase kinase-3, *Trends Biochem. Sci. 29*, 95–102.

20. Grimes, C.A., and Jope, R.S. (2001) The multifaceted roles of glycogen synthase kinase 3β in cellular signaling, *Prog. Neurobiol. 65*, 391–426.

21. Nikoulina, S.E., Ciaraldi, T.P., Mudaliar, S., Mohideen, P., Carter, L., and Henry, R.R. (2000) Potential role of glycogen synthase kinase-3 in skeletal muscle insulin resistance of type 2 diabetes, *Diabetes 49*, 263–271.

22. Takashima, A., Noguchi, K., Sato, K., Hoshino, T., and Imahori, K. (1993) Tau protein kinase I is essential for amyloid beta-protein-induced neurotoxicity, *Proc. Natl. Acad. Sci. USA 90*, 7789–7793.

23. Welsh, G.I., Patel, J.C., and Proud, C.G. (1997) Peptide substrates suitable for assaying glycogen synthase kinase-3 in crude cell extracts, *Anal. Biochem. 244*, 16–21.

24. Doble, B.W., and Woodgett, J.R. (2003) GSK-3: tricks of the trade for a multi-tasking kinase, *J. Cell. Sci. 116*, 1175–1186.

25. Brabek, J., and Hanks, S.K. (2004) Assaying protein kinase activity, *Methods Mol. Biol. 284*, 79–90.

26. Whitney, J.A. (2004) Reference systems for kinase drug discovery: chemical genetic approaches to cell-based assays, *Assay Drug Dev. Technol. 2*, 417–429.

27. Sadler, T.M., Achilleos, M., Ragunathan, S., Pitkin, A., LaRocque, J., Morin, J., Annable, R., Greenberger, L.M., Frost, P., and Zhang, Y. (2004) Development and comparison of two nonradioactive kinase assays for I kappa B kinase, *Anal. Biochem. 326*, 106–113.

28. Zaman, G.J., Garritsen, A., de Boer, T., and van Boeckel, C.A. (2003) Fluorescence assays for high-throughput screening of protein kinases, *Comb. Chem. High Throughput Screen. 6*, 313–320.

29. Sportsman, J.R., Daijo, J., and Gaudet, E.A. (2003) Fluorescence polarization assays in signal transduction discovery, *Comb. Chem. High Throughput Screen. 6*, 195–200.

30. Wenham, D., Illy, C., St. Pierre, J.A., and Bouchard, N. (2006) Development of high-throughput screening assays for kinase drug targets using AlphaScreen™ technology, *Drug Discov. Series 5*, 53–70.

31. Morgan, A.G., McCauley, T.J., Stanaitis, M.L., Mathrubutham, M., and Millis, S.Z. (2004) Development and validation of a fluorescence technology for both primary

and secondary screening of kinases that facilitates compound selectivity and site-specific inhibitor determination, *Assay Drug Dev. Technol. 2*, 171–181.

32. Loomans, E.E., van Doornmalen, A.M., Wat, J.W., and Zaman, G.J. (2003) High-throughput screening with immobilized metal ion affinity-based fluorescence polarization detection, a homogeneous assay for protein kinases, *Assay Drug Dev. Technol. 1*, 445–453.

33. Martin, K., Steinberg, T.H., Cooley, L.A., Gee, K.R., Beechem, J.M., and Patton, W.F. (2003) Quantitative analysis of protein phosphorylation status and protein kinase activity on microarrays using a novel fluorescent phosphorylation sensor dye, *Proteomics 3*, 1244–1255.

34. Cross, D. (2001) Assays for glycogen synthase kinase-3 (GSK-3), *Methods Mol. Biol. 124*, 147–159.

35. Burns, K.L., and May, S.W. (2003) Separation methods applicable to the evaluation of enzyme-inhibitor and enzyme-substrate interactions, *J. Chromatogr. B 797*, 175–190.

36. a) Wu, J., Takayama, S., Wong, C.-H., and Siuzdak, G. (1997) Quantitative electrospray mass spectrometry for the rapid assay of enzyme inhibitors, *Chem. Biol. 4*, 653–657; b) Bothner, B., Chavez, R., Wei, J., Strupp, C., Phung, Q., Schneemann, A., and Siuzdak, G. (2000) Monitoring enzyme catalysis with mass spectrometry, *J. Biol. Chem. 275*, 13455–13459; c) Shen, Z., Go. E.P., Gamez, A., Apon, J.V., Fokin, V., Greig, M., Ventura, M., Crowell, J.E., Blixt, O., Paulson, J.C., Stevens, R.C., Finn, M.G., and Siuzdak, G. (2004) A mass spectrometry plate reader: monitoring enzyme activity and inhibition with a Desorption/Ionization on Silicon (DIOS) platform, *Chembiochem. 5*, 921–927.

37. a) Lee, E.D., Mück, W., Henion, J.D., and Covey, T.R. (1989) Real-time reaction monitoring by continuous-introduction ion-spray tandem mass spectrometry, *J. Am. Chem. Soc. 111*, 4600–4604; b) Benetton, S., Kameoka, J., Tan, A., Wachs, T., Craighead, H., and Henion, J.D. (2003) Chip-based P450 drug metabolism coupled to electrospray ionization-mass spectrometry detection, *Anal. Chem. 75*, 6430–6436.

38. Lei, Q.P., Lamb, D.H., Heller, R.K., Shannon, A.G., Ryall, R., and Cash, P. (2002) Kinetic studies on the rate of hydrolysis of N-ethyl-N'-(dimethylaminopropyl)carbodiimide in aqueous solutions using mass spectrometry and capillary electrophoresis, *Anal. Biochem. 310*, 122–124.

39. Newton, R.P., Bayliss, M.A., Khan, J.A., Bastani, A., Wilkins, A.C., Games, D.E., Walton, T.J., Brenton, A.G., and Harris, F.M. (1999) Kinetic analysis of cyclic CMP-

specific and multifunctional phosphodiesterases by quantitative positive-ion fast-atom bombardment mass spectrometry, *Rapid Commun. Mass Spectrom. 13*, 574–584.

40. a) Ge, X., Sirich, T.L., Beyer, M.K., Desaire, H., and Leary, J.A. (2001) A strategy for the determination of enzyme kinetics using electrospray ionization with an ion trap mass spectrometer, *Anal. Chem. 73*, 5078–5082; b) Pi, N., Armstrong, J.I., Bertozzi, C.R., and Leary, J.A. (2002) Kinetic analysis of NodST sulfotransferase using an electrospray ionization mass spectrometry assay, *Biochemistry 41*, 13283–13288; c) Pi, N., Yu, Y., Mougous, J.D., and Leary, J.A. (2004) Observation of a hybrid random ping-pong mechanism of catalysis for NodST: a mass spectrometry approach, *Protein Sci. 13*, 903–912; d) Pi, N., Freel Meyers, C.L., Pacholec, M., Walsh, C.T., and Leary, J.A. (2004) Mass spectrometric characterization of a three-enzyme tandem reaction for assembly and modification of the novobiocin skeleton, *Proc. Natl. Acad. Sci. USA 101*, 10036–10041; e) Carroll, K.S., Gao, H., Chen, H., Stout, C.D., Leary, J.A., and Bertozzi, C.R. (2005) A conserved mechanism for sulfonucleotide reduction, *PLoS Biol. 3*, e250; f) Pi, N., Hoang, M.B., Gao, H., Mougous, J.D., Bertozzi, C.R., and Leary, J.A. (2005) Kinetic measurements and mechanism determination of Stf0 sulfotransferase using mass spectrometry, *Anal. Biochem. 341*, 94–104.

41. a) Min, D.-H., Tan, W.-J., and Mrksich, M. (2004) Chemical screening by mass spectrometry to identify inhibitors of anthrax lethal factor, *Nat. Biotechnol. 22*, 717–723; b) Min, D.-H., Su, J., and Mrksich, M. (2004) Profiling kinase activities by using a peptide chip and mass spectrometry, *Angew. Chem. Int. Ed. 43*, 5973–5977; c) Min, D.-H., Yeo, W.-S., and Mrksich, M. (2004) A method for connecting solution-phase enzyme activity assays with immobilized format analysis by mass spectrometry, *Anal. Chem. 76*, 3923–3929.

42. de Boer, A.R., Letzel, T., van Elswijk, D.A., Lingeman, H., Niessen, W.M., and Irth, H. (2004) On-line coupling of high-performance liquid chromatography to a continuous-flow enzyme assay based on electrospray ionization mass spectrometry, *Anal. Chem. 76*, 3155–3161.

43. Palm, A.K., and Novotny, M.V. (2005) A monolithic PNGase F enzyme microreactor enabling glycan mass mapping of glycoproteins by mass spectrometry, *Rapid Commun. Mass Spectrom. 19*, 1730–1738.

44. Zhang, B., Palcic, M.M., Schriemer, D.C., Alvarez-Manilla, G., Pierce, M., and Hindsgaul, O. (2001) Frontal affinity chromatography coupled to mass spectrometry for screening mixtures of enzyme inhibitors, *Anal. Biochem. 199*, 173–182.

45. Kelly, M.A., McLellan, T.J., and Rosner, P.J. (2002) Strategic use of affinity-based mass spectrometry techniques in the drug discovery process, *Anal. Chem. 74*, 1–9.

46. a) Dunayevskiy, Y.M., Lai, J.-J., Quinn, C., Talley, F., and Vouros, P. (1997) Mass spectrometric identification of ligands selected from combinatorial libraries using gel filtration, *Rapid Commun. Mass Spectrom. 11*, 1178–1184; b) Huyer, G., Kelly, J., Moffat, J., Zamboni, R., Jia, Z., Gresser, M.J., and Ramachandran, C. (1998) Affinity selection from peptide libraries to determine substrate specificity of protein tyrosine phosphatases, *Anal. Biochem. 258*, 19–30; c) Siegel, M.M., Tabei, K., Bebernitz, G.A., and Baum, E.Z. (1998) Rapid methods for screening low molecular mass compounds non-covalently bound to proteins using size exclusion and mass spectrometry applied to inhibitors of human cytomegalovirus protease, *J. Mass Spectrom. 33*, 264–273; d) Davis, R.G., Anderegg, R.J., and Blanchard, S.G. (1999) Iterative size-exclusion chromatography coupled with liquid chromatographic mass spectrometry to enrich and identify tight-binding ligands from complex mixtures, *Tetrahedron 55*, 11653–11667; e) Moy, F.J., Haraki, K., Mobilio, D., Walker, G., Powers, R., Tabei, K., Tong, H., and Siegel, M.M. (2001) MS/NMR: a structure-based approach for discovering protein ligands and for drug design by coupling size exclusion chromatography, mass spectrometry, and nuclear magnetic resonance spectroscopy, *Anal. Chem. 73*, 571–581.

47. a) Kaur, S., McGuire, L., Tang, D., Dollinger, G., and Heubner, V. (1997) Affinity selection and mass spectrometry-based strategies to identify lead compounds in combinatorial libraries, *J. Protein Chem. 16*, 505–511; b) Blom, K.F., Larsen, B.S., and McEwen, C.N. (1999) Determining affinity-selected ligands and estimating binding affinities by online size exclusion chromatography/liquid chromatography-mass spectrometry, *J. Comb. Chem. 1*, 82–90; c) Davidson, W., Hopkins, J.L., Jeanfavre, D.D., Barney, K.L., Kelly, T.A., and Grygon, C.A. (2003) Characterization of the allosteric inhibition of a protein-protein interaction by mass spectrometry, *J. Am. Soc. Mass Spectrom. 14*, 8–13; d) Annis, D.A., Athanasopoulos, J., Curran, P.J., Felsch, J.S., Kalghatgi, K., Lee, W.H., Nash, H.M., Orminati, J.-P.A., Rosner, K.E., Shipps, G.W. Jr., Thaddupathy, G.R.A., Tyler, A.N., Vilenchik, L., Wagner, C.R., and Wintner, E.A. (2004) An affinity selection–mass spectrometry method for the identification of small molecule ligands from self-encoded combinatorial libraries: discovery of a novel antagonist of *E.coli* dihydrofolate reductase, *Int. J. Mass Spectrom. 238*, 77–83.

48. a) Wieboldt, R., Zweigenbaum, J., and Henion, J. (1997) Immunoaffinity ultrafiltration with ion spray HPLC/MS for screening small-molecule libraries, *Anal. Chem. 69*, 1683–1691; b) Zhao, Y.-Z., van Breemen, R.B., Nikolic, D., Huang, C.-R., Woodbury, C.P., Schilling, A., and Venton, D.L. (1997) Screening solution-phase combinatorial libraries using pulsed ultrafiltration/electrospray mass spectrometry, *J. Med. Chem. 40*, 4006–4012.

49. a) Colton, I.J., Carbeck, J.D., Rao, J., and Whitesides, G.M. (1998) Affinity capillary electrophoresis: a physical-organic tool for studying interactions in biomolecular recognition, *Electrophoresis 19*, 367–382; b) Chu, Y.-H., Dunayevskiy, Y.M., Kirby,

D.P., Vouros, P., and Karger, B.L. (1996) Affinity capillary electrophoresis-mass spectrometry for screening combinatorial libraries, *J. Am. Chem. Soc. 118*, 7827–7835; c) Dunayevskiy, Y.M., Lyubarskaya, Y.V., Chu, Y.-H., Vouros, P., and Karger, B.L. (1998) Simultaneous measurement of nineteen binding constants of peptides to vancomycin using affinity capillary electrophoresis-mass spectrometry, *J. Med. Chem. 41*, 1201–1204.

50. a) Schriemer, D.C., Bundle, D.R., Li, L., and Hindsgaul, O. (1998) Micro-scale frontal affinity chromatography with mass spectrometric detection: a new method for the screening of compound libraries, *Angew. Chem. Int. Ed. 37*, 3383–3387; b) Schriemer, D.C. (2004) Biosensor alternative: frontal affinity chromatography, *Anal. Chem. 76*, 440A-448A; c) Slon-Usakiewicz, J.J., Ng, W., Dai, J.-R., Pasternak, A., and Redden, P.R. (2005) Frontal affinity chromatography with MS detection (FAC-MS) in drug discovery, *Drug Discov. Today 10*, 409–416.

51. de Boer, A.R., Letzel, T., Lingeman, H., and Irth, H. (2005) Systematic development of an enzymatic phosphorylation assay compatible with mass spectrometric detection, *Anal. Bioanal. Chem. 381*, 647–655.

52. Bowley, E., Mulvihill, E., Howard, J.C., Pak, B.J., Gan, B.S., and O'Gorman, D.B. (2005) A novel mass spectrometry-based assay for GSK-3β activity, *BMC Biochem. 6*, 29.

53. Fundamentals of Enzyme Kinetics, Cornish-Bowden, A.; Buterworthy, Toronto; 1977, pp. 152-174.

54. Zhang, J.H., Chung, T.D., and Oldenburg, K.R. (1999) A simple statistical parameter for use in evaluation and validation of high throughput screening assays, *J. Biomol. Screen. 4*, 67–73.

55. Ozbal, C.C., LaMarr, W.A., Linton, J.R., Green, D.F., Katz, A., Morrison, T.B., and Brenan, C.J. (2004) High throughput screening via mass spectrometry: a case study using acetylcholinesterase, *Assay Drug Develop. Technol. 2*, 373–381.

Chapter 3

Preliminary Characterization of Sol-gel Entrapped GSK-3β

This chapter was based on work that was solely performed by me with input and direction from Dr. Brennan. Dr. Werstuck assisted me in the proper training required for performing radioisotope-based assays. I wrote the first draft of the manuscript and Dr. Brennan provided editorial input to generate the final draft of the paper.

Abstract

Herein we describe preliminary studies on the entrapment of GSK-3β within DGS-derived sol-gel materials. Solid-state assays involving sol-gel derived materials have previously been shown to generate reproducible and accurate enzymatic activity data. The incorporation of GSK-3β into sol-gel derived materials has not been demonstrated, and was the key objective of this work. Entrapment of this enzyme was done first in sol-gel derived bulk glasses in 96-well plates. A radioassay was then used to evaluate the extent of protein leaching from the macroporous silica matrix, revealing a minimal extent of leaching. However, the non-specific binding (NSB) problem that is innate to the interaction between negatively charged silica and positively charged substrate/product species was noted as an obstacle to efficient substrate/product diffusion, thus rendering activity tests difficult. Preliminary steps to overcome the NSB problem are discussed. NSB was evaluated using blank sol-gel columns with known ATP-competitive inhibitors of GSK-3. Compounds tested demonstrated at least some degree of NSB. Assessment of GSK-3β activity using affinity methods in silica did not show proper interaction between the inhibitor and enzyme, suggesting potential denaturation/ inactivation of the kinase in sol-gel.

3.1 Introduction

Solid-phase assays offer a number of advantages in the field of drug screening, such as access to various assays formats (FAC/MS, bioSPME) that are not possible in solution, reusability of costly protein and dependable assay automation.[1] Hence, the development of a solid-phase assay utilizing GSK-3β was explored. For this purpose, GSK-3β was

entrapped in sol-gel derived materials and assessed for assay development. Previous examples of successful enzyme entrapment in sol-gel derived materials provided a good starting point for this process. For example, the determination of K_m values for the substrates of dihydrofolate reductase (DHFR), Factor Xa, COX-II and γ-GT as well as of K_I values for their inhibitors was achieved using mesoporous protein-doped sol-gel monoliths in 96-well plates.[2] In all experiments, the results were comparable with data obtained in solution assays, differing by no more than a factor of 3. Protein-doped columns containing nicotinic acetylcholine receptor (nACHR)[3] and a fluorescein antibody[4] were used to generate the K_d values for epibatidine and fluorescein, respectively. Also, a small scale mixture screen using entrapped adenosine deaminase (ADA) in a DGS-derived sol-gel column was able to discern a specific inhibitor of the enzyme out of a mixture of 49 compounds using the continuous flow IMER/MS assay method[1]. The versatility of the proteins amenable to sol-gel entrapment as well as the accuracy of sol-gel-based assays suggest that this emerging technology will play an important role not only in enzyme characterization, but also in enzyme inhibitor screening in the future.

In order to acquire binding affinity data for GSK-3β, an inhibitor-based frontal affinity chromatography (FAC/MS) binding site assay[5,6] can be applied, through the use of the strong ATP-competitive inhibitor SB-415286 (ligand) and the anionic indicator molecule, fluorescein (void marker). FAC/MS relies on retention time to characterize binding, with strong inhibitors binding quickly to the protein and saturating the column, resulting in signal delay. Once a strong inhibitor equilibrates in the column, the signal

slowly plateaus. In contrast, weak inhibitors, at the same concentration, will not have many binding sites accessible and will elute quickly (Fig. 3.1).

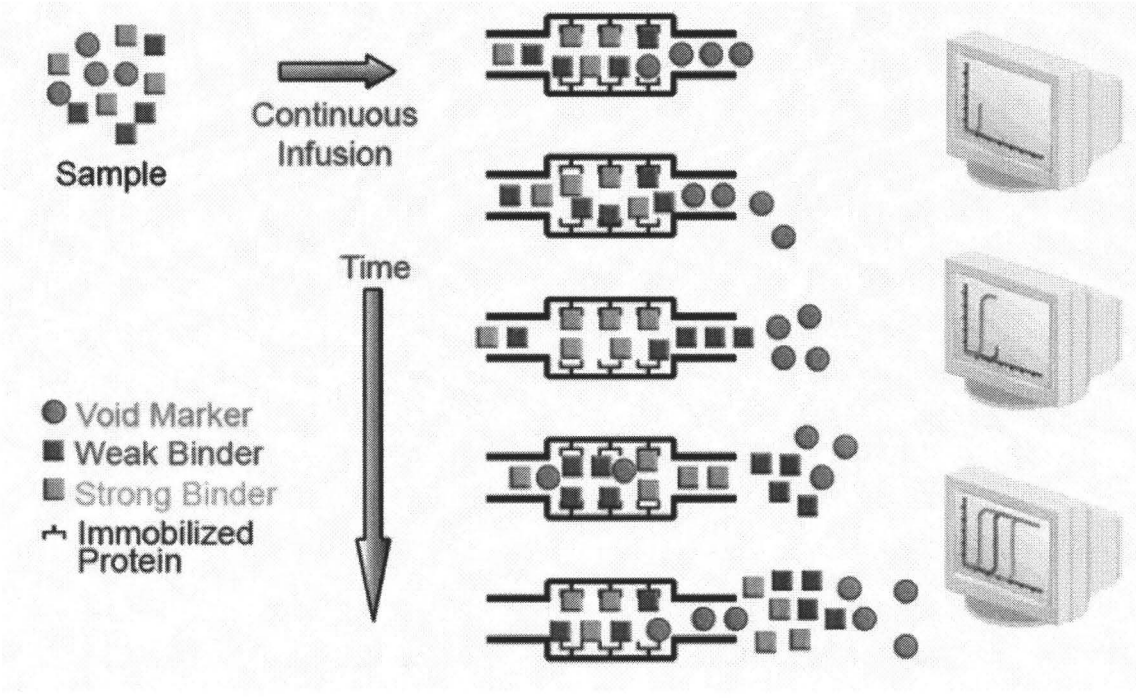

Figure 3.1: Diagram of a FAC/MS assay. Following the void marker, weak binders elute quickly. Retention is greater for strong binders, resulting in longer elution time (Figure originally published in Slon-Usakiewicz, J.J. et al., 2005, *Drug Discov. Today*[7]).

Therefore, by plotting the inhibitor concentration versus its corresponding elution volume for a range of SB-415286 concentrations and using the formula

$$V - V_0 = \frac{B_t}{(K_d + [L])} \qquad (3)$$

where V is the elution time of ligand, V_0 is the elution time of void marker and [L] is the inhibitor concentration, the amount of protein immobilized (B_t) and the dissociation constant (K_d) can be determined.

The goals of this study were: 1) the characterization of GSK-3β leaching in macroporous sol-gel monoliths; 2) the assessment of non-specific binding (NSB) to silica; and 3) GSK-3β-specific retention for the purpose of developing an affinity based solid-phase assay for this protein. The leaching and activity of sol-gel entrapped GSK-3β from DGS-derived sol-gel monoliths is investigated through the use of a radiolabeled product peptide, the quantity of which is measured continuously over a number of washes of the monoliths. The presence of NSB between substrate/product/inhibitors and the silica matrix is discussed. Kinase-doped sol-gel columns are then utilized in FAC/MS experiments designed to evaluate the interaction of known inhibitors with the entrapped protein and to gauge the applicability of this approach to drug screening.

3.2 Experimental Section

3.2.1 Materials

Magnesium acetate, adenosine 5'-triphosphate (ATP), histidine-tagged recombinant rabbit glycogen synthase kinase 3β (GSK-3β) (15 units/μg protein where 1 unit will transfer one pmol of phosphate from ATP to phosphatase inhibitor 2 per min at pH 7.5 at 30°C), fluorescein, SB-415286 and 10 kDa poly(ethylene glycol) (PEG) were purchased from Sigma-Aldrich (Oakville, Ontario, Canada). 1-Azakenpaullone and GSK-3β Inhibitor VIII were purchased from Calbiochem (San Diego, California, USA). Ammonium acetate, 4-(2-Hydroxyethyl) piperazine-1-ethanesulfonic acid (HEPES), HPLC grade water and acetone were purchased from Caledon Laboratory Chemicals (Georgetown, Ontario, Canada). Synthetic muscle glycogen synthase 1 peptide (GSM) (structure: Arg-Arg-Arg-Pro-Ala-Ser-Val-Pro-Pro-Ser-Pro-Ser-Leu-Ser-Arg-His-Ser-pSer-His-Gln-Arg-Arg (2673 Da, pSer = phosphoserine)) was purchased from Upstate

USA (Charlottesville, VA, USA). [γ-^{32}P]-ATP and ACS aqueous scintillation cocktail were obtained from GE Healthcare Bio-Sciences (Baie d'Urfe, Quebec, Canada). 85% *o*-phosphoric acid was obtained from Fisher Scientific (Nepean, Ontario, Canada). Diglycerylsilane (DGS) was prepared by methods described elsewhere[8] using tetramethylorthosilicate (Sigma-Aldrich) and anhydrous glycerol (Fisher Scientific). Fused silica tubing was purchased from Polymicro Technologies (Phoenix, AZ, USA). C96 microwell plates were purchased from VWR International (Mississauga, Ontario, Canada). All reagents were used as received.

3.2.2 Fabrication of GSK-3β Sol-gel Monoliths in 96-well Plates

8 μL of 2.1 μM GSK-3β in 20 mM Tris buffer, pH 7.5 was mixed with 4 μL of a solution containing 400 mM HEPES, pH 7.0. DGS based sols were prepared by sonicating DGS with water (1 g + 1 mL) at 0 °C for 15 min to hydrolyze the monomer, followed by filtration through a 0.2 μm filter. 20 μL of the resulting sol was rapidly mixed with the 12 μL GSK-3β solution prepared above, followed by the rapid addition of 8 μL of 25% (w/v) PEG in water. The sol solution was then placed into wells of polystyrene 96 well plates (well volume: 350 μL/well). After gelation, 96 well plates were stored at 4 °C and aged for a minimum of 4 days to achieve a relatively stable internal structure within the monoliths.

3.2.3 GSK-3β Radioassays of Leaching

GSK-3β at a final concentration of 420 nM, was entrapped in sol-gel monoliths in 96-well plates, followed by washes with 6 mM NH_4OAc/0.8 mM MgOAc buffer for 20 min

intervals (0 – 120 min). GSM (62.5 μM) and 125 μM 0.5 μCi/μl [γ-^{32}P]-ATP were then added to the washes and were incubated for 1 h in a total volume of 40 μL. The monolith was treated with 62.5 μM GSM, 125 μM 0.5 μCi/μl [γ-^{32}P]-ATP and 6 mM NH_4OAc/0.8 mM MgOAc buffer and allowed to incubate for 1 h in a total volume of 40 μL. After 1 h, the samples were spotted onto Whatman P81 phosphocellulose papers and washed three times with 0.75% *o*-phosphoric acid and once with acetone. The unbound [γ-^{32}P]-ATP was washed away in the process, leaving only the radio labeled pGSM produced during the enzyme incubation bound to the paper, allowing quantification of the product by scintillation counting.

3.2.4 Fabrication of GSK-3β Columns

12.5 μL of 2.1 μM GSK-3β in 20 mM Tris buffer, pH 7.5 was mixed with 12.5 μL of a solution containing 400 mM HEPES, pH 7.0. DGS based sols were prepared by sonicating DGS with water (1 g + 1 mL) at 0 °C for 15 min to hydrolyze the monomer, followed by filtration through a 0.2 μm filter. 50 μL of the resulting sol was rapidly mixed with the 25 μL of the GSK-3β solution prepared above (in the case of blank columns, 25 μL 400 mM HEPES, pH 7.0 was used instead), followed by the rapid addition of 25 μL of 20% (w/v) PEG in water. The sol solution was then injected into a 40 cm length of 250 μm ID, 360 μm OD, polyimide coated fused silica tubing. The liquid sol must be completely mixed, injected and stationary within the capillary by the time phase separation occurs, ~2 minutes after mixing. After gelation (~ 3 min), capillaries were looped such that both ends could be submerged in 50 mM HEPES, pH 7.0, and

secured for storage. Columns were aged for a minimum of 3 days to achieve a relatively stable internal structure.

3.2.5 Column Handling

Prior to experiments, a fresh 40 cm long column (~20 μL internal volume) was equilibrated off-line, with mobile phase from a syringe pump (Harvard Instruments model 22), to remove aqueous poly(ethylene glycol) and glycerol. New columns were connected to the pump using 75 μm ID fused silica tubing and another 75 μm ID tubing segment was attached to the bottom of the column using Upchurch Microtight unions (Oak Harbor, WA, USA). Several bed volumes of mobile phase were passed through the column at 0.5 μL/min before slowly increasing the flow rate to 10 μL/min. Columns were attached directly to the Turbospray ion source of an AB/Sciex Q-Trap mass spectrometer with 75 μm ID fused silica tubing.

3.2.6 LC/MS Settings

Mobile phase delivery for substrate/product signal optimization studies was performed with a 1.0 mL, 4.6 mm ID Hamilton syringe, using an AB/Sciex Q-Trap Mass Spectrometer syringe pump controlled by Analyst v.1.4 software. Mass spectrometer control and data acquisition were performed with Analyst v.1.4 software. Precursor-product ion pairs were followed using the multiple reaction monitoring (MRM) mode in positive ion mode under the following conditions: Curtain Gas = 45.0, Collision gas = high, Ion Spray Voltage = 5000 V, Temperature = 175 °C, Ion Source Gas 1 = 40.0, Ion

Source Gas 2 = 40.0. Specific MS/MS parameters for each ion pair are provided in Table 3.1. The total scan time was 5 seconds per point.

3.2.7 Sol-gel Non-specific Binding Assay

Blank sol-gel columns of 10-cm length were prepared following the procedure outlined above. Non-specific binding of the inhibitors was then assessed through the injection of a mixture of 10 μM SB-415286, GSK-3β Inhibitor VIII and 1-Azakenpaullone with 1 μM fluorescein through the columns at 5 μL/min. Inhibitor interaction with the enzyme was measured using 50 nM and 10 nM SB-415286 inhibitor with 500 nM fluorescein void marker, injected through the 10-cm 262.5 nM GSK-3β-doped columns at a rate of 5 mL/min using the Eksigent NanoLC pump. In all cases, the makeup flow (used to assist in the generation of a stable electrospray) consisted of methanol and was delivered at 5 μL/min with the syringe pump, resulting in a total flow rate of 10 μL/min entering the ESI-MS. The mass spectrometer was operated in multiple reaction monitoring mode with simultaneous detection of *m/z* 309 → 120 (GSK-3β Inhibitor VIII); 360 → 154 (SB-415286); 328 → 220 (1-Azakenpaullone) and 333 → 287 (fluorescein). For specific compound MS settings, refer to Table 3.1.

Species	Q1 (m/z)	Q3 (m/z)	DP (V)	EP (V)	CE (V)	CXP (V)
Fluorescein	333	287	80	8	44	3
1-Azakenpaullone	328	220	75	10	52	2.5
GSK-3β Inhibitor VIII	309	120	40	6	15	4
SB-415286	360	154	50	10	25	5

Table 3.1: Specific MS/MS parameters for each compound ion pair. The total scan time was 5 seconds per point.

3.3 Results and Discussion

3.3.1 Optimization of Sol-gel Entrapped GSK-3β Performance

An important goal of the GSK-3β studies was to determine the entrapped enzyme's interaction with its sol-gel environment through the assessment of various criteria such as the quantity of GSK-3β leached from sol-gel monoliths as well as its activity in sol-gel. These studies were of particular interest due to their relevance in revealing the applicability of sol-gel column entrapped GSK-3β to on-line inhibitor screening. Using macroporous GSK-3β-doped sol-gel monoliths as a model system, enzyme leaching was examined first to determine its contribution to potential activity loss in sol-gel.

Fig. 3.2 (top panel) demonstrates a decline in the quantity of leaching over a 2 h period, as represented by the decrease in turnover from 1.5% (first wash) to 0.4% (last wash), indicating a low quantity of active GSK-3β present in the wash solutions. The

turnover of 2.7% produced within the monolith (initially loaded with 1.40 μg of protein) during the 1 h incubation period following the washes was also low, given the solution assay value of 5.1% produced with a protein content of 0.18 μg (Fig 2.3). Assessing the cumulative enzyme activity in the washes (Fig. 3.2, bottom panel) revealed a low value of 2.1 μM pGSM/μg GSK-3β or 11.3% as normalized to the activity obtained in the solution radio assay in Fig. 2.3 (18.4 μM/μg). The activity in the post-wash monolith was measured at 1.2 μM/μg or 6.6%, implying possible deactivation of GSK-3β during the sol-gel synthesis as the reason behind low activity in the washes and monolith. Another possible cause of this problem may have been NSB that occurred between the negatively charged silica matrix and the highly positively charged substrate and product peptides, due to the relatively low ionic strength of the buffer. NSB could thus act as a deterrent to GSM diffusion in, and pGSM diffusion out, of the monolith, restricting the detectable pGSM to extremely small concentrations. To accommodate for NSB and to eliminate this effect, neutralization of the charge on the silica surface within the monolith was required.

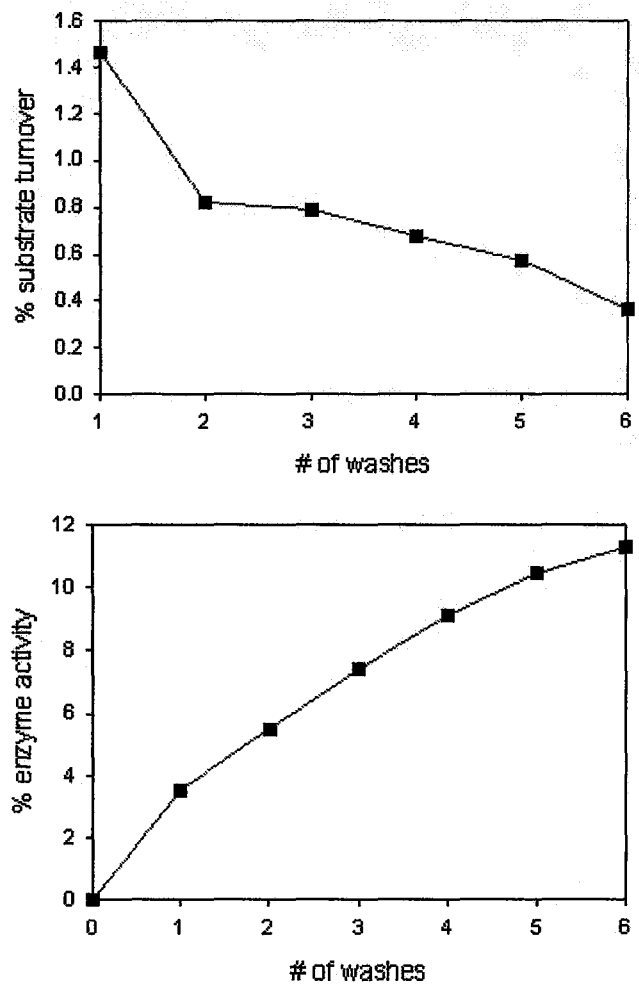

Figure 3.2: GSK-3β sol-gel leaching analysis with ^{32}P-ATP radioassay. % substrate turnover (pGSM (μM)/total GSM in reaction (μM)) obtained from 20 min washes with 6 mM NH_4OAc/0.8 mM MgOAc, pH 7.4 buffer (top) and cumulative enzyme activity over the 2 h wash period (μM pGSM/μg GSK-3β normalized to enzyme activity in solution) (bottom).

In an attempt to resolve the problem of NSB, the experiment was repeated with a post-wash treatment of the monolith with 1 M KCl. The high concentration of salt applied for 1 h following the washes would dissociate any silica bound pGSM owing to the high ionic strength of KCl. The extent of turnover in this assay was again low, going from 3.1% to 0.3% (Fig. 3.3, top panel), with the turnover produced in the monolith after the washes at 2.1%, despite the high salt treatment. The cumulative enzyme activity for the washes was similar to the previous assay with 2.4 μM/μg or 13.0% and the post-wash

monolith activity was recorded to be 0.93 μM/μg or 5.1% (Fig. 3.3, bottom panel). Utilization of KCl, was thus inadequate to resolve the NSB issue, possibly because this approach involved only post-wash application. Although any bound pGSM was removed, it was not possible to improve the access of the substrate to the enzyme during the reaction. Treatment of the monolith after the reaction may be insufficient, as the substrate may be unable to enter the enzyme's active site for conversion, resulting in low product quantity.

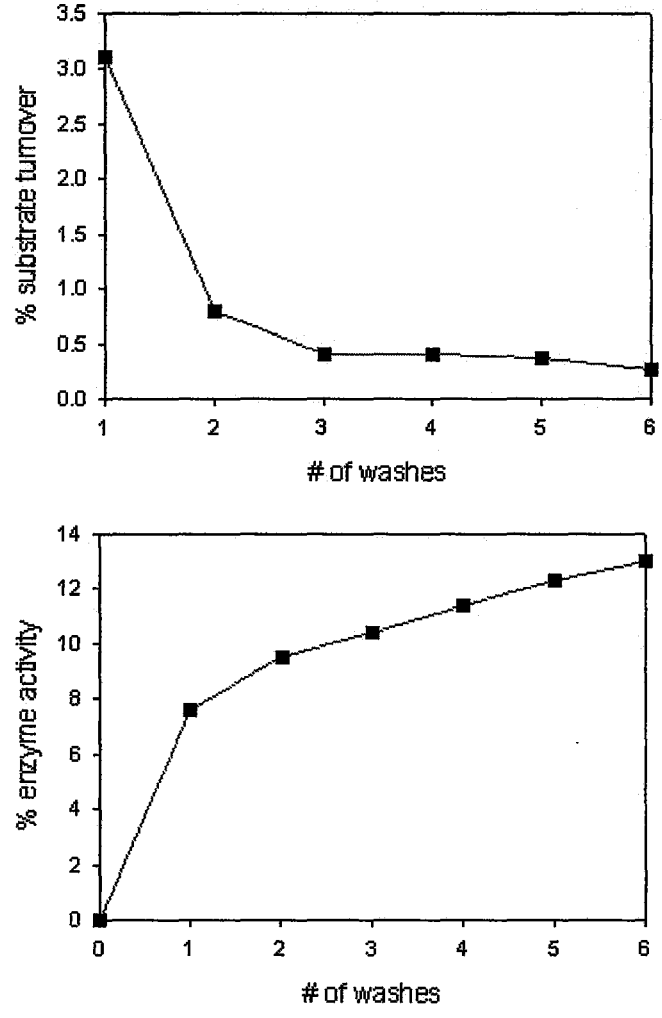

Figure 3.3: Radio assay GSK-3β sol-gel leaching analysis with 1 M KCl high salt wash. % substrate turnover (pGSM (μM)/total GSM in reaction (μM)) obtained from 20 min washes with 6 mM NH_4OAc/0.8 mM MgOAc, pH 7.4 buffer (top) and cumulative enzyme activity over the 2 h wash period (μM pGSM/μg GSK-3β normalized to enzyme activity in solution) (bottom).

3.3.2 GSK-3β Inhibitor Retention Assay

Due to the difficulties stemming from the strong non-specific interactions of substrate and product with silica, an alternative means of kinase activity quantification was devised in order to successfully characterize sol-gel entrapped GSK-3β. The first step in this procedure required the acquisition of ESI-MS signals for known potent ATP-competitive inhibitors that would bind reliably to the enzyme – 1-Azakenpaullone, GSK-3β Inhibitor VIII and SB-415286. The specific MRM transitions for these compounds were determined and parameters optimized for their effective monitoring (Table 3.1). During preliminary scans, SB-415286 demonstrated the highest ionization and signal, indicating good detectability of the compound and exhibiting potential for subsequent FAC/MS assays.

After establishing optimal MRM transitions for the ATP-competitive inhibitors, they were tested for NSB to the negatively charged silica matrix of sol-gel columns. This was required since NSB can result in the retention of these compounds by the silica within the column, altering elution times and leading to false assessments of inhibitor-protein interactions. A mixture of 10 μM 1-Azakenpaullone, GSK-3β Inhibitor VIII, SB-415286 and 1 μM fluorescein (void marker as it will not interact with the silica due to its negative charge) were run through a blank sol-gel column at 5 μL/min for 20 min. The resulting data traces in Fig. 3.4 show little retention for GSK-3β Inhibitor VIII and SB-415286 with the simultaneous and rapid breakthrough time of the compounds closely matching that of the void marker, fluorescein (~3 min). Non-specific binding, however, was demonstrated by the inhibitor 1-Azakenpaullone, which exhibited a longer retention time compared to the other compounds. Subsequently, due to its high MRM mode signal and

the absence of substantial NSB to the silica, SB-415286 was selected as the indicator compound of choice for use with GSK-3β-doped sol-gel columns.

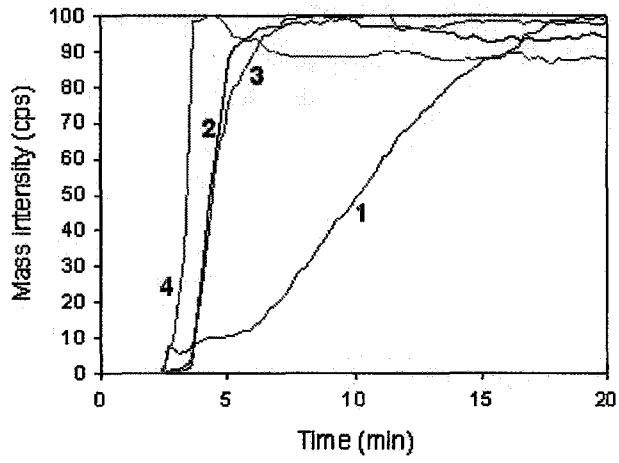

Figure 3.4: Normalized assessment of GSK-3β inhibitor non-specific retention within blank sol-gel columns. 10 μM 1-Azakenpaullone (red, 1), GSK-3β Inhibitor VIII (blue, 2), SB-415286 (pink, 3) and 1 μM fluorescein (green, 4), all dissolved in 6 mM NH_4OAc/0.8 mM MgOAc, pH 7.4 buffer were injected at 5 μL/min for 20 min.

Following the characterization of the inhibitory compounds, the interaction of sol-gel entrapped GSK-3β with SB-415286 was examined. The first breakthrough curve was acquired for 50 nM SB-415286 in an assay run with 500 nM fluorescein (void marker) in buffer for 16 min in a 15 cm column with an initial loading of 26.3 pmol of GSK-3β (Fig. 3.5, top panel). The breakthrough time obtained for fluorescein was approximately 10 min, while SB-415286 did not appear to fully break through until 12 min. Although this discrepancy was initially attributed to the binding of the compound to GSK-3β, a follow-up assay with 10 nM SB-415286 demonstrated the same breakthrough time for both compounds (Fig. 3.5, bottom panel). This was not expected, as the decrease in ligand concentration should have resulted in a longer breakthrough time for SB-415286. Relative to the 50 nM concentration, 10 nM SB-415286 contains fewer molecules available for binding site saturation and was expected to demonstrate a time dependent

shift in its breakthrough time. Since the elution time did not increase with the concentration drop, the absence of specific inhibitor retention of SB-415286 with GSK-3β became evident. As this lack of inhibitor interaction with the ATP binding site may have been caused by the denaturation of GSK-3β upon its entrapment in sol-gel, FAC/MS assays and affinity inhibitor screens would not be amenable to this system. Further modification of this method to increase enzyme stability is necessary to continue GSK-3β sol-gel studies.

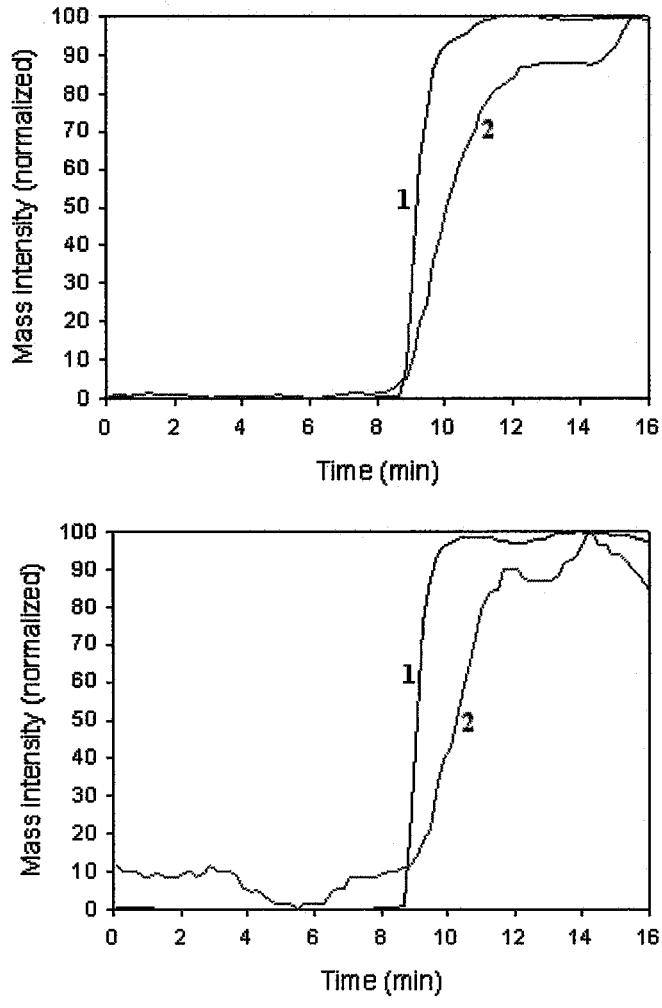

Figure 3.5: Inhibitor binding assay with 500 nM fluorescein (blue, 1)/50 nM SB-415286 (red, 2) (top) and 500 nM fluorescein (blue, 1)/10 nM SB-415286 (red, 2) (bottom).

3.4 Conclusions

The GSK-3β sol-gel studies yielded substantial information on the behaviour of this enzyme within the confines of a silica matrix. While entrapment of this kinase in monoliths did not demonstrate significant leaching of active enzyme over a series of washes, as determined by the near-absence of activity in the samples, NSB proved to be a substantial obstacle to overcome. Treating the sol-gel with KCl after the washes did not increase detectable enzyme activity, as it could only affect the diffusion of pGSM out of the monolith and could not increase GSM diffusion into the monolith prior to the washes. Selection of the optimal compound for affinity based activity assays revealed SB-415286, an ATP-competitive inhibitor, to possess the highest signal in MRM mode with minimal NSB to silica. Application of this inhibitor in a FAC/MS assay revealed no binding to the GSK-3β trapped inside the sol-gel column, suggesting denaturation of the enzyme. However, work done by J. Lebert using mesoporous silica materials with entrapped GSK-3β, revealed a fully functional enzyme within the sol-gel monoliths (unpublished data). Although these results can in part be attributed to the co-entrapment of substrate with the kinase in the sol-gel material, it does raise the possibility of eliciting enzyme activity within more macroporous silica monoliths and columns. Other kinases shown to function within sol-gel include Src kinase[9], protein kinase A[10] and creatine kinase[11], suggesting that GSK-3β may be retained as an active enzyme in sol-gel materials. Further studies in this field will require the evaluation of the interaction between surface modifying agents, such as APTES, and GSK-3β in a sol-gel environment as well as the comparison of enzyme leaching and activity in mesoporous and macroporous sol-gel materials.

3.6 References

1. Hodgson, R.J., Besanger, T.R., Brook, M.A., and Brennan, J.D. (2005) Inhibitor screening using immobilized enzyme-reactor chromatography/mass spectrometry, *Anal. Chem. 77*, 7512–7519.

2. Besanger, T.R., Chen, Y., Deisingh, A.K., Hodgson, R.J., Jin, W., Mayer, S., Brook, M.A., and Brennan, J.D. (2003) Screening of inhibitors using enzymes entrapped in sol-gel-derived materials, *Anal. Chem. 75*, 2382–2391.

3. Besanger, T.R., Hodgson, R.J., Guillon, D., and Brennan, J.D. (2006) Monolithic membrane-receptor columns: optimization of column performance for frontal affinity chromatography/mass spectrometry applications, *Anal. Chim. Acta 561*, 107–118.

4. Hodgson, R.J., Brook, M.A., and Brennan, J.D. (2005) Capillary-scale monolithic immunoaffinity columns for immunoextraction with in-line laser-induced fluorescence detection, *Anal. Chem. 77*, 4404–4412.

5. Schriemer, D.C., Bundle, D.R., Li, L., and Hindsgaul, O. (1998) Micro-scale frontal affinity chromatography with mass spectrometric detection: a new method for the screening of compound libraries, *Angew. Chem. Int. Ed. 37*, 3383–3387.

6. Ng, W., Dai, J.-R., Slon-Usakiewicz, J., Redden, P.R., Pasternak, A., and Reid, N. (2007) Automated multiple ligand screening by frontal affinity chromatography-mass spectrometry (FAC-MS), *J. Biomol. Screen. 12*, 167–174.

7. Slon-Usakiewicz, J.J., Ng, W., Dai, J.R., Pasternak, A., and Redden, P.R. (2005) Frontal affinity chromatography with MS-detection (FAC-MS) in drug discovery, *Drug Discov. Today 10*, 409–416.

8. Brook, M.A., Chen, Y., Guo, K., Zhang, Z., and Brennan, J.D. (2004) Sugar-modified silanes: precursors for silica monoliths, *J. Mater. Chem. 14*, 1469–1479.

9. Cruz-Aguado, J.A., Chen, Y., Zhang, Z., Brook, M.A., and Brennan, J.D. (2004) Entrapment of Src protein tyrosine kinase in sugar-modified silica, *Anal. Chem. 76*, 4182–4188.

10. Rupcich, N., Green, J.R., and Brennan, J.D. (2005) Nanovolume kinase inhibition assay using a sol-gel-derived multicomponent microarray, *Anal. Chem. 77*, 8013–8019.

11. Lan, E.H., Dunn, B., and Zink, J.I. (2005) Nanostructured systems for biological materials, *Methods Mol. Biol. 300*, 53–79.

Chapter 4

Conclusions and Future Outlook

4.1 Conclusions

Through the application of the ESI-MS/MS detection technology to solution-based GSK-3β assays, an improved method for monitoring multiply phosphorylated peptides was developed, optimized and applied towards kinase inhibitor screening. As a unique system, the MS kinase assay first required optimization of operational parameters in both the solution reaction conditions and instrument detection settings, as discussed in Chapter 2. Since ionized magnesium salt contributes to signal suppression in electrospray mass spectrometers, a calibration experiment was done in order to determine the tolerance of the GSK-3β substrate signal to a gradient of Mg^{2+} concentrations. As expected, the extent of the charge stealing increased proportionally to the amount of salt present, leaving a window between 0.8 and 1.6 mM MgOAc for acceptable signal detection, with 37 – 19% of the control signal intensity remaining. Prior to commencing with MS work however, an extensive analysis with ^{32}P radioassays was performed to obtain the minimal functional concentrations of Mg^{2+} and buffer. The data yielded values of 0.8 mM MgOAc and 6 mM NH_4OAc, which corresponded well with the established threshold of ESI-MS tolerance for ion suppression. The newly acquired protocol was then tested in a standard ^{32}P radio assay, where it showed good protein activity, converting ~11% of the substrate in 2 h.

The assay was then tested with ESI-MS/MS detection in order to obtain IC_{50} values for a few known GSK-3β inhibitors, with the intent to characterize their respective modes

of action. By varying ATP and GSM levels that induced shifts in the IC_{50}s, the expected modes of inhibition were confirmed as being ATP-competitive (SB-415286) and allosteric (GSK-3β Inhibitor I & GSK-3β Inhibitor II), demonstrating the utility of this method for secondary screen hit confirmation. When examining assay reproducibility, a statistical validation of the solution-based ESI-MS/MS approach was conducted, providing a Z' value of 0.68. With the semi-automated ESI-MS/MS mixture screening method, a Z' value of 0.60 was obtained. These Z' values indicate substantial statistical relevance of the hits generated by this approach. Although applying this technology to screening a 100 compound library against GSK-3β did not yield any new hits, this method nevertheless proved its capacity for hit detection by responding to the presence of a spiked inhibitor in one of the mixtures, followed by its successful deconvolution from the mixture. Taking this early proof-of-concept data into consideration, it is apparent that MS based inhibitor screening has a significant potential for future development and implementation of this technique into fully automated systems that can screen vast chemical compound libraries and natural product extracts.

In Chapter 3, the focus of the thesis shifted to the development of ESI-MS/MS in conjunction with sol-gel immobilized GSK-3β as a viable alternative to solution-based assays, with the key goal of acquiring enzyme reusability through the use of sol-gel materials. The initial step in this direction involved the examination of protein leaching from sol-gel monoliths and was assessed with the ^{32}P radioassay method. The quantity of active leached enzyme was low as cumulative activity from the washes was only 11.3% of solution control. The amount of substrate conversion fell from 1.5% in the first wash to 0.4% in the last wash with the activity of the remaining enzyme in the monolith at

2.7% (6.6% activity). Although absence of activity in the monolith assay may have been due to the inactivity of enzyme in silica, it was also possible that such low product yield from the monolith was the result of electrostatic interactions between the positively charged GSM/pGSM and the negatively charged silica. Introduction of KCl to disrupt these interactions did not improve the results, as cumulative substrate activity was 13.0% and monolith activity was 5.1%. Due to this restriction, performing IMER/MS assays with the aim of monitoring enzyme activity in real-time would be problematic without prior surface modification of the silica.

Due to the problems with non-specific binding, we decided to pursue an affinity based screening route using small organic molecules instead, as they were considerably less likely to exhibit non-specific binding to sol-gel. After performing the necessary MS calibration for three ATP-competitive inhibitors to improve their signal, they were subjected to an NSB test, where along with fluorescein as the void marker, they were flushed through a blank sol-gel column. While SB-415286 and GSK-3β Inhibitor VIII showed no interaction with the solid phase, 1-Azakenpaullone did have substantial NSB, and was dropped from the list of usable compounds for this assay. Owing to its higher signal and better ionization, SB-415286 was selected as the inhibitor that would be applied in the affinity based assay. However, when flushed through at 50 and 10 nM concentrations through a sol-gel column with trapped GSK-3β, no enzyme-specific retention of this molecule was observed.

A potential cause of this may have been high leaching in the column, caused by the strong backpressure created within a continuous flow system, which has been shown to cause a substantial loss of binding capacity and retention. Equally possible, the silica

entrapment process may have denatured or concealed GSK-3β from the inhibitor, resulting in problems with the assay. Future studies in this field will be required to resolve a number of issues, namely the extent of leaching of GSK-3β in sol-gel columns, the effect of silica gelation on enzyme stability and the reduction of non-specific binding. Further inquisition into the material properties of sol-gel should uncover the means to both reduce leaching and effectively eliminate unwanted interactions with the silica. Protein activity can potentially be improved through the utilization of sugar-modified silanes during the casting of the sol-gel columns.

4.2 Future Outlook

The research presented in this thesis demonstrates the applicability of an electrospray mass spectrometry detection method for solution-based GSK-3β activity assays to allow mixture screening. Although substantial progress has been made in this area, many hurdles remain to be overcome prior to the implementation of this procedure to a full scale high-throughput screen. A primary issue that requires resolution is the optimization of the solvent constitution to allow both good compound solubility and high MS signal of the substrate/product. An important aspect to consider for this task would be the extent of the hydrophobicity of solvents containing the compounds from a library/natural product extract. A useful solvent would be both, hydrophilic to avoid phase separation from the aqueous buffer used in the enzyme reactions, and non-toxic to the enzyme in order to avoid unwanted inhibition which would create a large number of false positives. The amount of compounds present in a mixture would also need to be optimized as to arrive at the lowest possible individual concentration with the highest possible number of ligands per sample. Time per assay is another aspect that requires improvement, as

increasing throughput of this method requires the shortening of sample processing periods. Once the ESI-MS limit of sensitivity is established, numerous compounds synthesized around functional scaffolds as well as organic molecule extracts from plants could be analyzed in a rapid and effective fashion.

Sol-gel immobilization of GSK-3β was not as straightforward as anticipated, but the continued development of this system should certainly be pursued, since an entrapped protein would be considerably more cost effective in the long run. The challenges remaining to be solved include: 1) The elimination of non-specific charge interactions between substrate/product and silica through surface modification; 2) Decreasing the extent of kinase leaching from columns under continuous flow by controlling sol-gel porosity; and 3) Attempting to raise enzyme stability in sol-gel with the addition of stabilizing compounds such as sugar-modified silanes. Following the utilization of the aforementioned improvements, solid phase immobilized GSK-3β would then become amenable to both affinity assays and IMER screening.